Acta Cryst B
STRUCTURAL SCIENCE
CRYSTAL ENGINEERING
MATERIALS

April 2022 issue

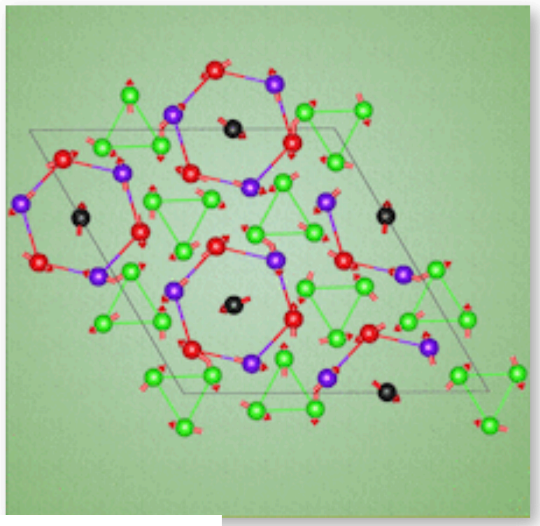

Cover illustration View of the magnetic Tb atoms of antiferrom
P6′ symmetry [see Pomjakushin *et al.* (2022). *Acta Cryst.* B**78**, 1

Revisiting the antiferromagnetic structure of $Tb_{14}Ag_{51}$: the importance of distinguishing alternative symmetries for a multidimensional order parameter

Vladimir Pomjakushin,[a]* Juan Manuel Perez-Mato,[b] Peter Fischer,[a] Lukas Keller[a] and Wiesława Sikora[c]

[a]Laboratory for Neutron Scattering and Imaging (LNS), Paul Scherrer Institut (PSI), CH-5232 Villigen, Switzerland, [b]Facultad de Ciencia y Tecnologa, Universidad del Pas Vasco, UPV/EHU, Apartado 644, E-48080 Bilbao, Spain, and [c]Faculty of Physics and Applied Computer Science, AGH University of Science and Technology, PL-30-059 Krakow, Poland. *Correspondence e-mail: vladimir.pomjakushin@psi.ch

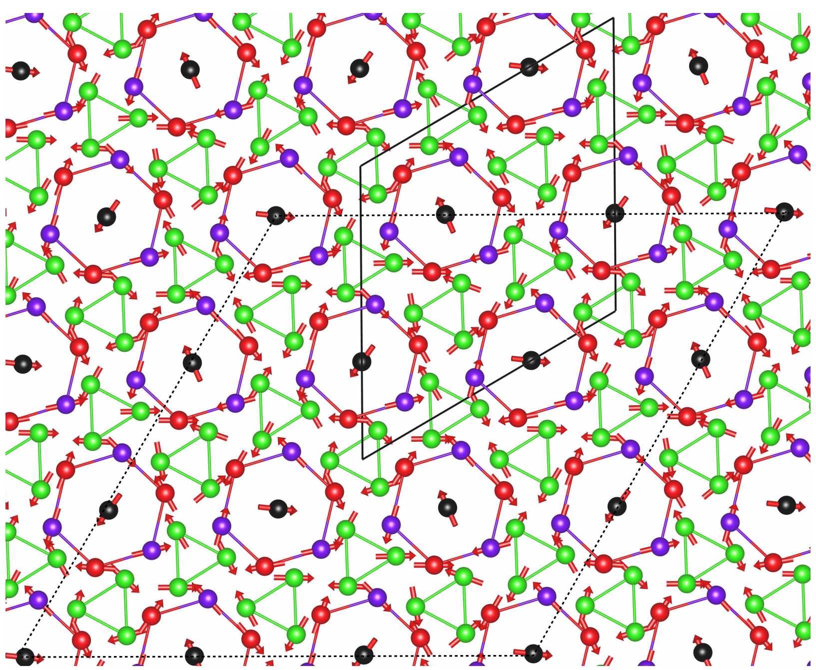

https://onlinelibrary.wiley.com/iucr/doi/10.1107/S205252062200124X#

15’+5’

Plan

Plan

- History behind the paper
  - Initial motivation to study magnetic structure of $Tb_{14}Ag_{51}$
  - Experiments at SINQ DMC and HRPT – 2004
  - Magnetic structure published in 2006

  - Manuel Perez–Mato idea: high symmetry lost 2014–,… 2019

Plan

- History behind the paper
  - Initial motivation to study magnetic structure of $Tb_{14}Ag_{51}$
  - Experiments at SINQ DMC and HRPT – 2004
  - Magnetic structure published in 2006

  - Manuel Perez–Mato idea: high symmetry lost 2014–,… 2019

- Herring criterion of the irreducible representations (irrep) type. Complex irreps.
- Alternative symmetries in case of multi-dim irreps

Plan

- History behind the paper
  - Initial motivation to study magnetic structure of $Tb_{14}Ag_{51}$
  - Experiments at SINQ DMC and HRPT – 2004
  - Magnetic structure published in 2006

  - Manuel Perez–Mato idea: high symmetry lost 2014–,… 2019

- Herring criterion of the irreducible representations (irrep) type. Complex irreps.
- Alternative symmetries in case of multi-dim irreps

- Neutron diffraction: new much better model for magnetic structure of $Tb_{14}Ag_{51}$

Initial motivation to study Tb14Ag51 in 1990…

Hexagonal P6/m space group

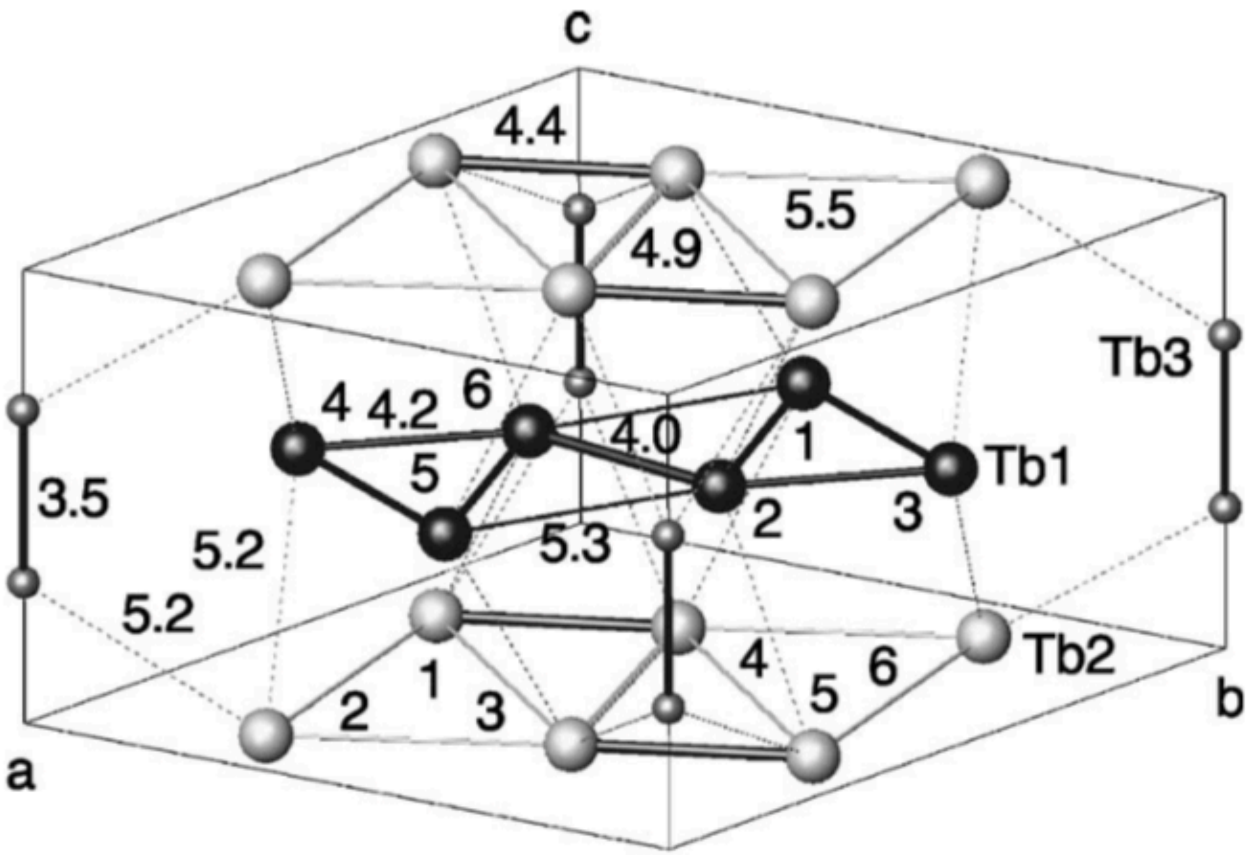

Tb1	6*k*
Tb2	6*j*
Tb3	2*e*

In actinides $U_{14}Au_{51}$ the f−electrons which carry the magnetism can participate in the Fermi surface

complex electronic properties like heavy−fermion behaviour, superconductivity and antiferromagnetism (AFM).

?

In which extent AFM ordering is different in $Tb_{14}Ag_{51}$ and in particular to investigate whether there may be also magnetic order on all rare−earth sites?

Interesting features of geometrically frustrated Tb14Ag51

- Textbook-like example of VERY complex magnetic structure: 27 parameters, 15 if M=const.

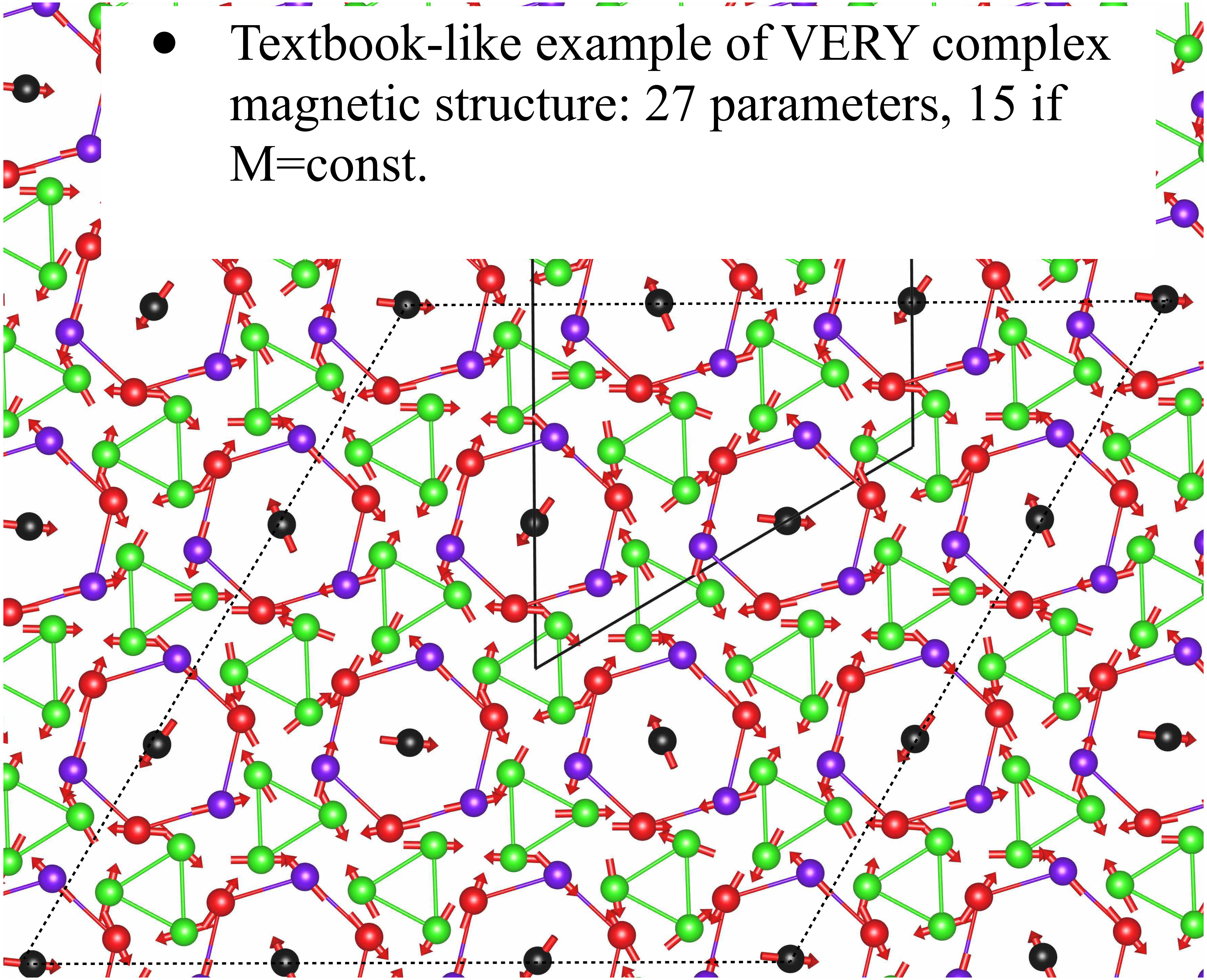

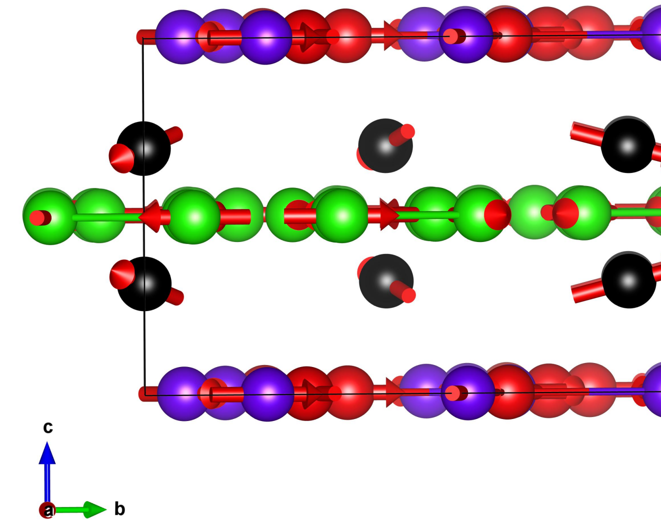

Interesting features of geometrically frustrated Tb14Ag51

- Textbook-like example of VERY complex magnetic structure: 27 parameters, 15 if M=const.

- spontaneous electric polarization induced by a noncollinear AFM ordering

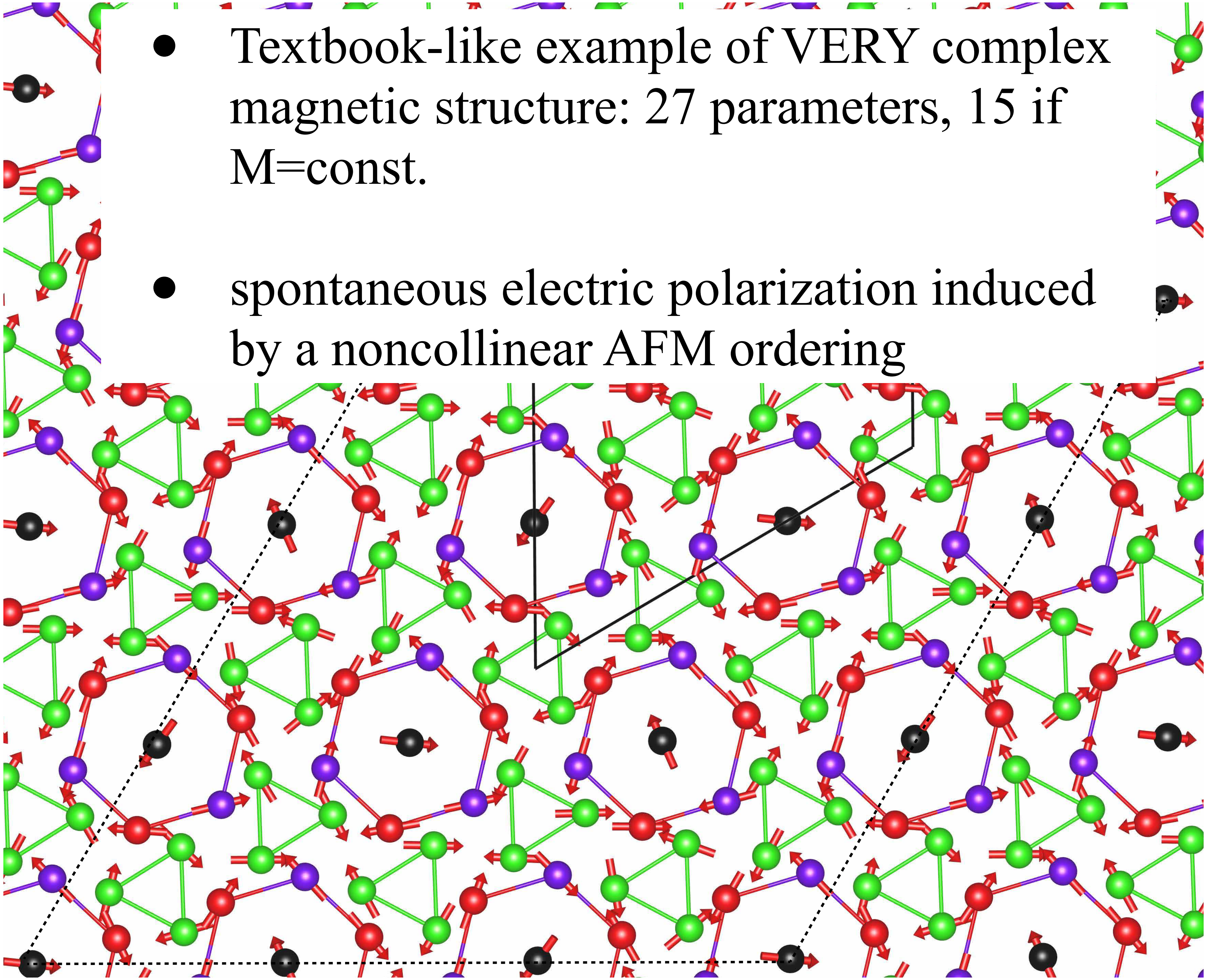

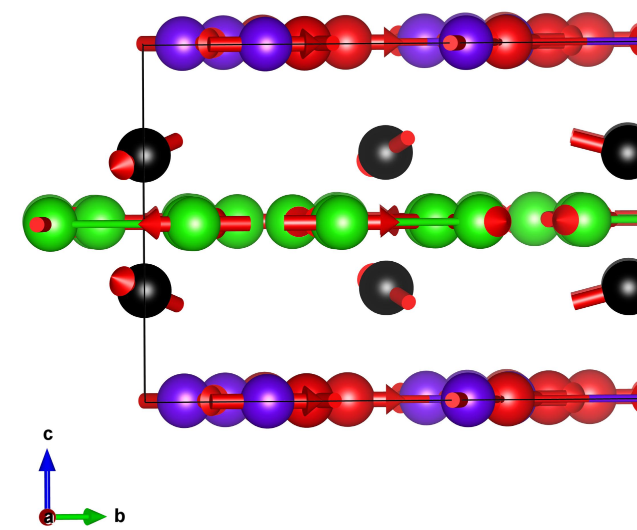

Interesting features of geometrically frustrated Tb14Ag51

- Textbook-like example of VERY complex magnetic structure: 27 parameters, 15 if M=const.

- spontaneous electric polarization induced by a noncollinear AFM ordering

  Vortex spin configuration allows exotic multipoles★ (important for spintronics):

- ferroic time-reversal-odd polar-tensor quantities, like ferromagnetic toroidicity (**r** x **M**)
- ferroaxial moment with time-reversal even and space inversion even (**r** x **Q**)

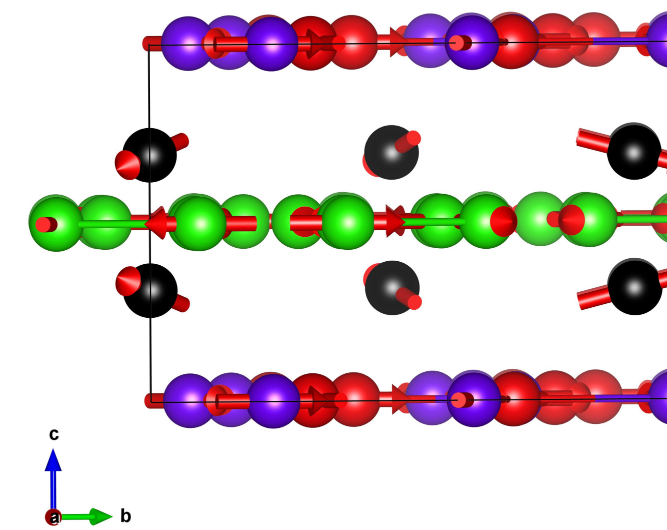

★ Satoru Hayami, PHYSICAL REVIEW B 106, 144402 (2022)

The materials hosting the vortex spin configurations in in some specific symmetries with exotic multipoles

New experiments at SINQ/DMC&HRPT 2003−2004

PHYSICAL REVIEW B **72**, 134413 (2005)

Antiferromagnetic three-sublattice Tb ordering in $Tb_{14}Ag_{51}$

P. Fischer,[1,*] V. Pomjakushin,[1] L. Keller,[1] A. Daoud-Aladine,[1] W. Sikora,[2] A. Dommann,[3,†] and F. Hulliger[3]
[1]*Laboratory for Neutron Scattering, ETH Zurich & Paul Scherrer Institute, CH-5232 Villigen PSI, Switzerland*
[2]*Faculty of Physics and Applied Computer Science, AGH University of Science and Technology, PL-30-059 Krakow, Poland*
[3]*Laboratory for Solid State Physics, ETH Hönggerberg, CH-8093 Zurich, Switzerland*
(Received 23 March 2005; revised manuscript received 16 May 2005; published 12 October 2005)

Bulk magnetic, x-ray, and neutron-diffraction measurements were performed on polycrystalline $Tb_{14}Ag_{51}$ in the temperature range from 1.5 K to room temperature. Its chemical $Gd_{14}Ag_{51}$-type structure corresponding to space group $P6/m$ has been refined at 300 and at 30 K. Combined with group-theoretical symmetry analysis, we show that the magnetic structure of this intermetallic compound is of a different $\mathbf{k}=(1/3,1/3,0)$ type with three magnetic Tb sublattices ordering simultaneously below $T_N=27.5(5)$ K according to the combined irreducible representations τ_4 and τ_6.

DOI: 10.1103/PhysRevB.72.134413 PACS number(s): 75.25.+z, 61.12.Ld, 71.20.Eh

I. INTRODUCTION

Intermetallic uranium and rare-earth $A_{14}B_{51}$ compounds with $Gd_{14}Ag_{51}$ structure[1] have interesting physical properties such as coexistence of antiferromagnetic order and heavy-fermion behavior in $Ce_{14}X_{51}$ (X=Au,Ag,Cu),[2] and in $U_{14}Au_{51}$.[3–5] This is related to the fact that there are three crystallographically distinct A sites in this structure.

Moreover, its particular hexagonal symmetry, due to quasitriangular arrangement of magnetic ions, gives rise to considerable geometric frustrations in the magnetic interactions.

diffraction data and performed a careful analysis of both the chemical and magnetic structures of $Tb_{14}Ag_{51}$. In particular we shall prove that in $Tb_{14}Ag_{51}$ the magnetic ordering is of a different type in the important class of intermetallic $A_{14}B_{51}$ compounds with remarkable variation of physical properties. In contrast to the heavy fermion system $U_{14}Au_{51}$,[4] in $Tb_{14}Ag_{51}$ all three A sublattices are shown to order magnetically below $T_N=27.5(5)$ K.

We also measured zero-field μSR spectra of the powder sample of $Tb_{14}Ag_{51}$ at the GPS spectrometer of Paul Scherrer Institute at 5, 20, and at 30 K. Unfortunately, in contrast to

magnetic susceptibility and I(T)

k−vector: k_K=[1/3, 1/3, 0]

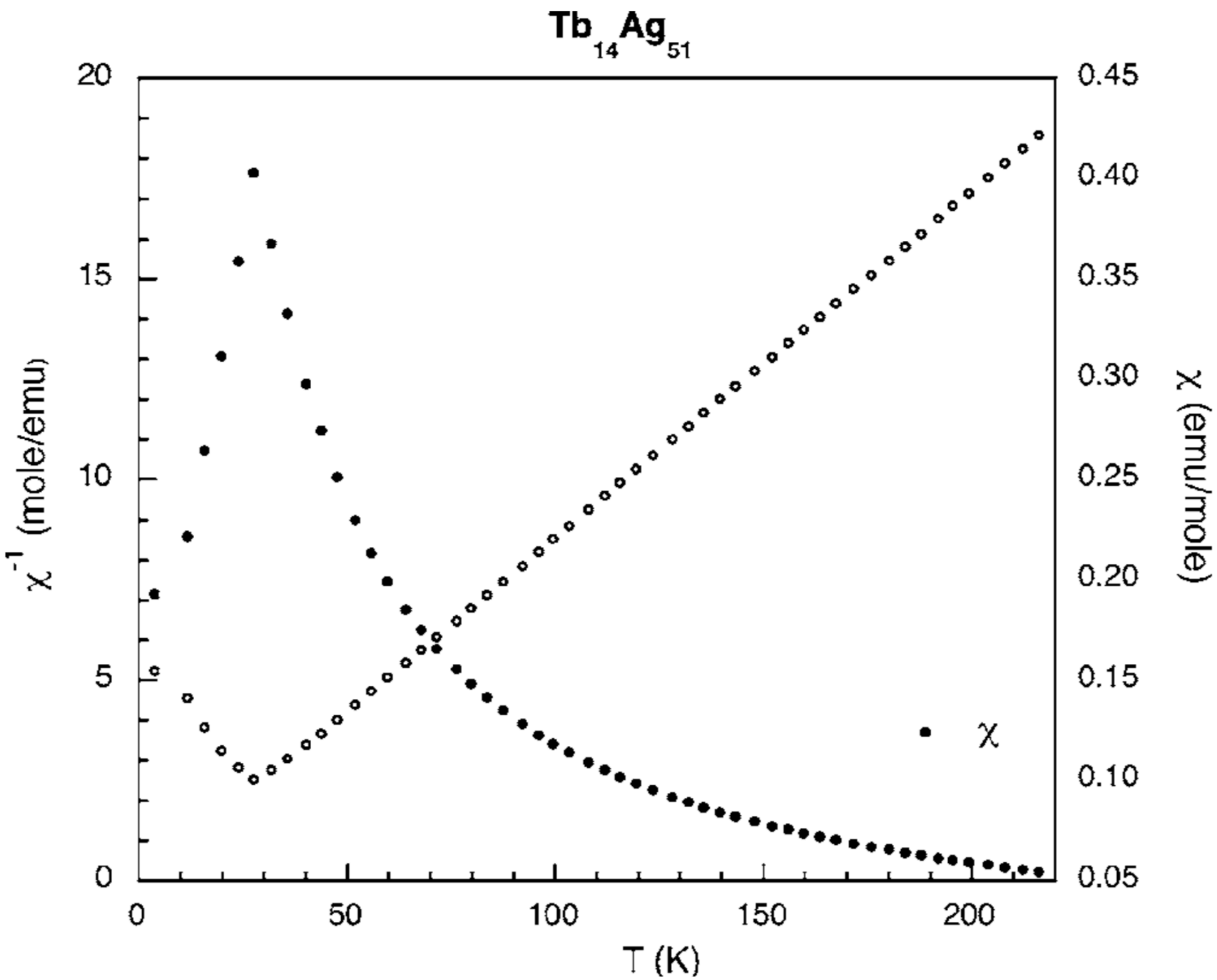

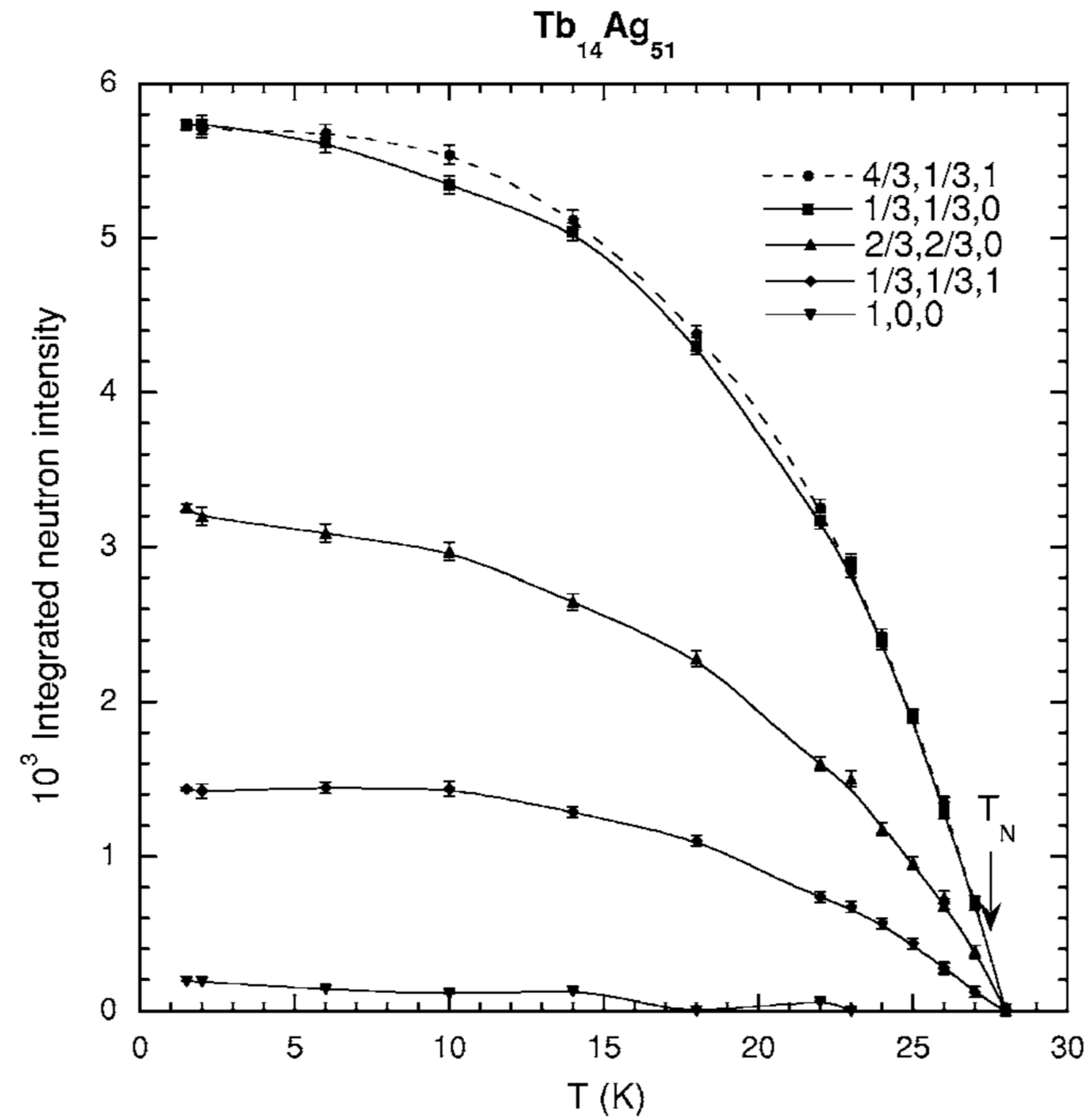

9.67_B / Tb was found to be close to the free ion value 9.72_B / Tb of Tb^{3+} with $^7F_6$ ground state.

FIG. 5. Temperature dependences of the integrated magnetic neutron intensities of characteristic magnetic Bragg peaks of $Tb_{14}Ag_{51}$. The smooth curves are a guide to the eyes.

2k magnetic structure was missed using RA

Antiferromagnetic (à la cycloidal spiral) three sub−lattice ordering in $Tb_{14}Ag_{51}$

P6/m → Pm' (lowest monoclinic symmetry)

k−vector: k_K=[1/3, 1/3, 0]

PHYSICAL REVIEW B 72, 134413 (2005)

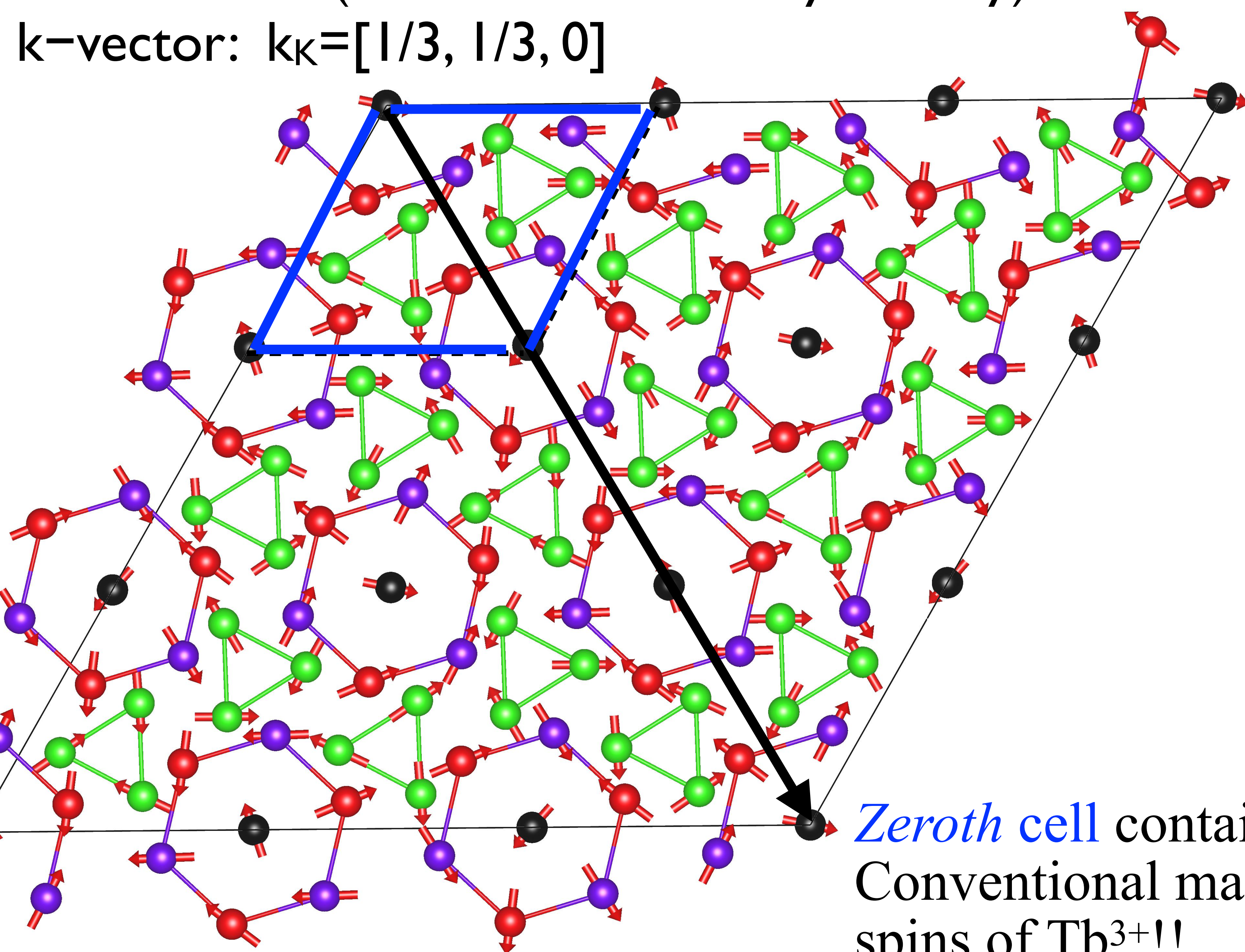

Zeroth cell contains 13 spins of Tb^{3+}.
Conventional magnetic unit cell contains 126 spins of Tb^{3+}!!

2k magnetic structure was missed using RA

Antiferromagnetic (à la cycloidal spiral) three sub−lattice ordering in $Tb_{14}Ag_{51}$

P6/m → Pm' (lowest monoclinic symmetry)

k−vector: k_K=[1/3, 1/3, 0]

PHYSICAL REVIEW B 72, 134413 (2005)

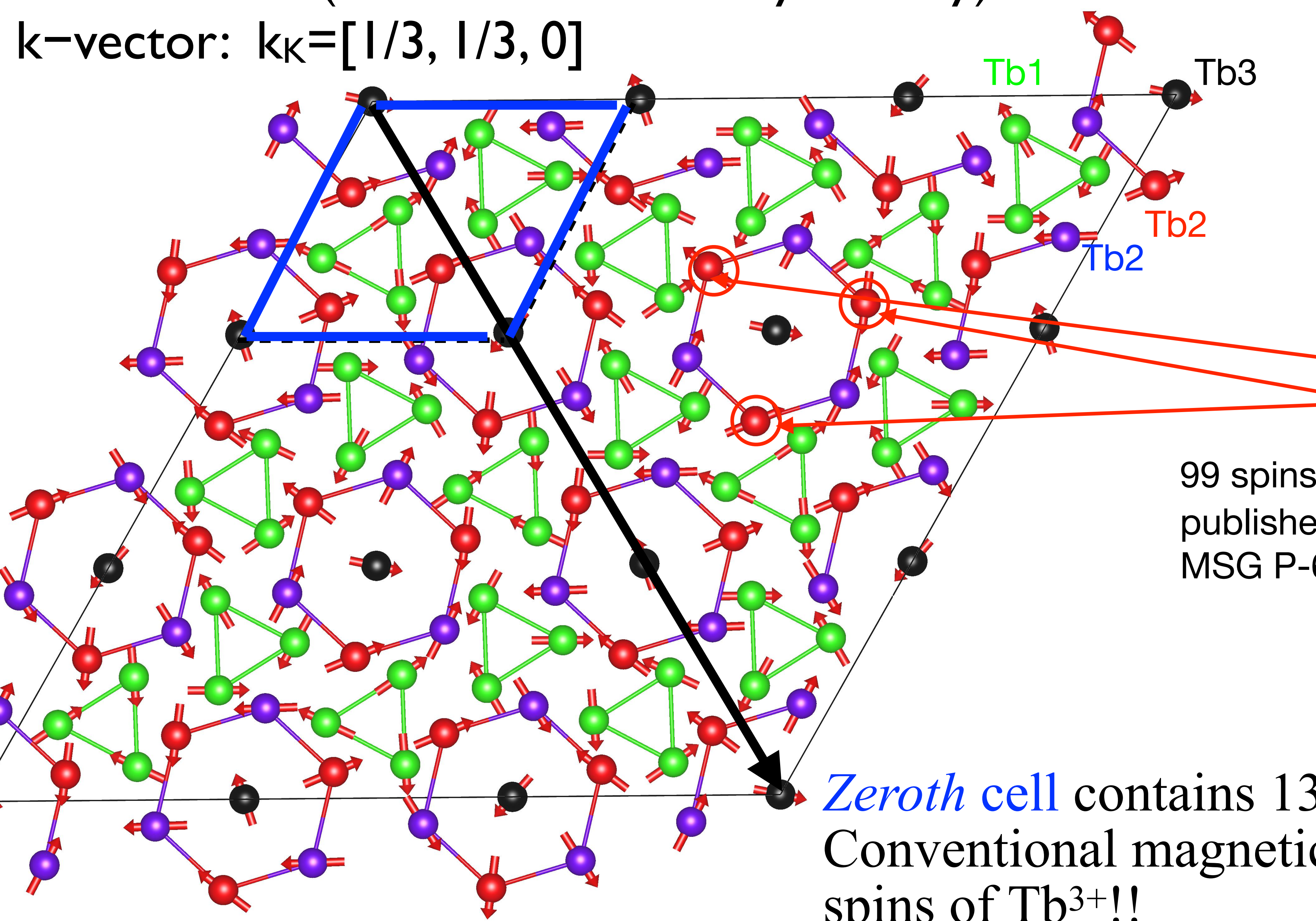

Manuel Perez Mato

Only three of 13 independent sites are “wrong” => Pm’

99 spins in the 3 x 3 x 1 cell of the published model comply with the MSG P-6’, while 27 do not.

Zeroth cell contains 13 spins of Tb^{3+}. Conventional magnetic unit cell contains 126 spins of Tb^{3+}!!

2k magnetic structure was missed using RA

Antiferromagnetic (à la cycloidal spiral) three sub−lattice ordering (irrep K4K6) in $Tb_{14}Ag_{51}$

P6/m → Pm' (lowest monoclinic symmetry)

k−vector: k_K=[1/3, 1/3, 0]

PHYSICAL REVIEW B 72, 134413 (2005)

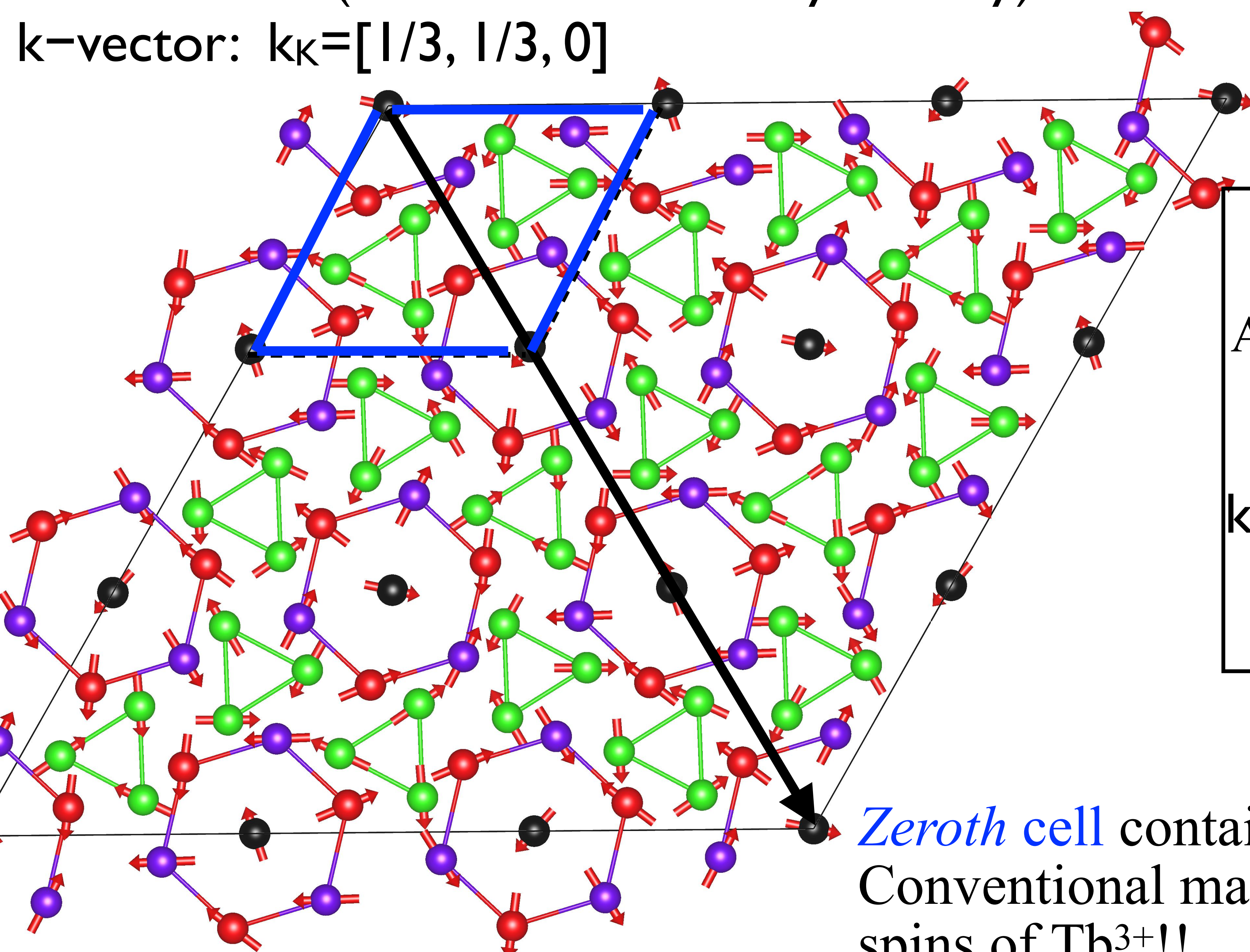

maximal possible symmetry for 4D irrep

Acta Cryst. (2022). B**78**, 172-178

P6/m → P-6'

k−vectors: k_K=[1/3, 1/3, 0] and $3k_K$=[0,0,0]

Zeroth cell contains 13 spins of Tb^{3+}.
Conventional magnetic unit cell contains 126 spins of Tb^{3+}!!

Energy Bands of Crystals and Types of irreps.

AUGUST 15, 1937 PHYSICAL REVIEW VOLUME 52

Conyers Herring

Herring in 1959

Effect of Time-Reversal Symmetry on Energy Bands of Crystals

CONYERS HERRING
Princeton University, Princeton, New Jersey
(Received June 16, 1937)

GUST 15, 1937 PHYSICAL REVIEW V

Accidental Degeneracy in the Energy Bands of Crystals

CONYERS HERRING
Princeton University, Princeton, New Jersey
(Received June 16, 1937)

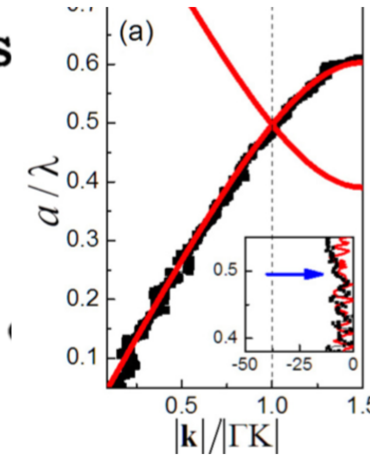

PhysRevB.89.134302

Wigner in 1963

E. Wigner: The degeneracies, such as touching or crossing the branches, are connected with the properties of the irreps of the spatial symmetry group of the Hamiltonian.
Three types of irreps – real & two complex.

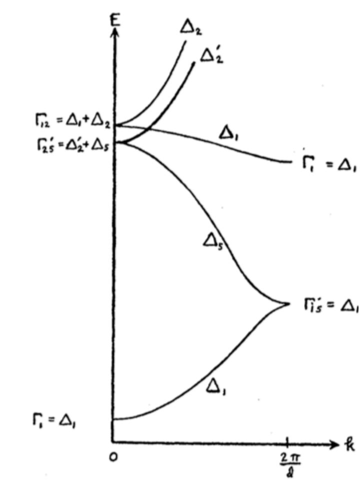

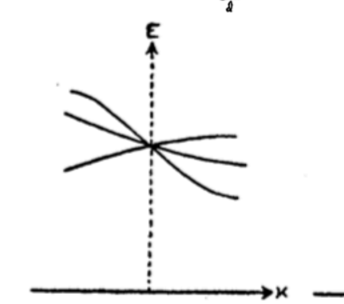

(A)

if H is real:
$E(\psi) = E(\psi^*)$

$\psi \rightarrow \psi^*$
is to be interpreted as
|same state>
Alice x,y,z → Bob x,y,z
t → –t

C. Herring PhD thesis: "On Energy Coincidences in the Theory of Brillouin Zones" (1937) under supervision of Eugene Wigner

Herring criterium is routinely used in crystallography for analysis of magnetic and crystal structures

Herring criterium for classification of irreducible representations (irreps) of the space groups

$$\eta = \frac{l_k}{n(G^0)} \sum_{\substack{h \\ h\mathbf{k} \backsim -\mathbf{k}}} \chi^{\kappa\nu}(g^2) = \begin{cases} 1, & \text{if } d^{\kappa\nu} \text{ is real,} \\ 0, & \text{if } d^{\kappa\nu} \text{ is complex and } d^{\kappa\nu} \nsim (d^{\kappa\nu})^*, \\ -1, & \text{if } d^{\kappa\nu} \text{ is complex and } d^{\kappa\nu} \backsim (d^{\kappa\nu})^*. \end{cases}$$

character

$g=\{h|\tau_h\}$

real, type 1

complex, type 3

pseudoreal, type 2

the irreducible representation matrices d^{kv}

Herring criterium for classification of irreducible representations (irreps) of the space groups

$$\eta = \frac{l_k}{n(G^0)} \sum_{\substack{h \\ h\mathbf{k} \backsim -\mathbf{k} \\ g=\{h|\tau_h\}}} \chi^{\kappa\nu}(g^2) = \begin{cases} 1, & \text{if } d^{\kappa\nu} \text{ is real,} \\ 0, & \text{if } d^{\kappa\nu} \text{ is complex and } d^{\kappa\nu} \nsim (d^{\kappa\nu})^*, \\ -1, & \text{if } d^{\kappa\nu} \text{ is complex and } d^{\kappa\nu} \backsim (d^{\kappa\nu})^*. \end{cases}$$

character

real, type 1

complex, type 3

pseudoreal, type 2

the irreducible representation matrices $d^{k\nu}$

Type3: Making use of the condition that quantities of physics must be real, the basis $\psi^{k\nu}$ of the representation $d^{k\nu}$ must be joined with the basis $(\psi^{k\nu})^*$ of the representation $(d^{k\nu})^*$ Such a reducible representation $d^{k\nu} \oplus (d^{k\nu})^*$ is termed irreducible in terms of physics.

representation approach to the magnetic structure in Tb14Ag51

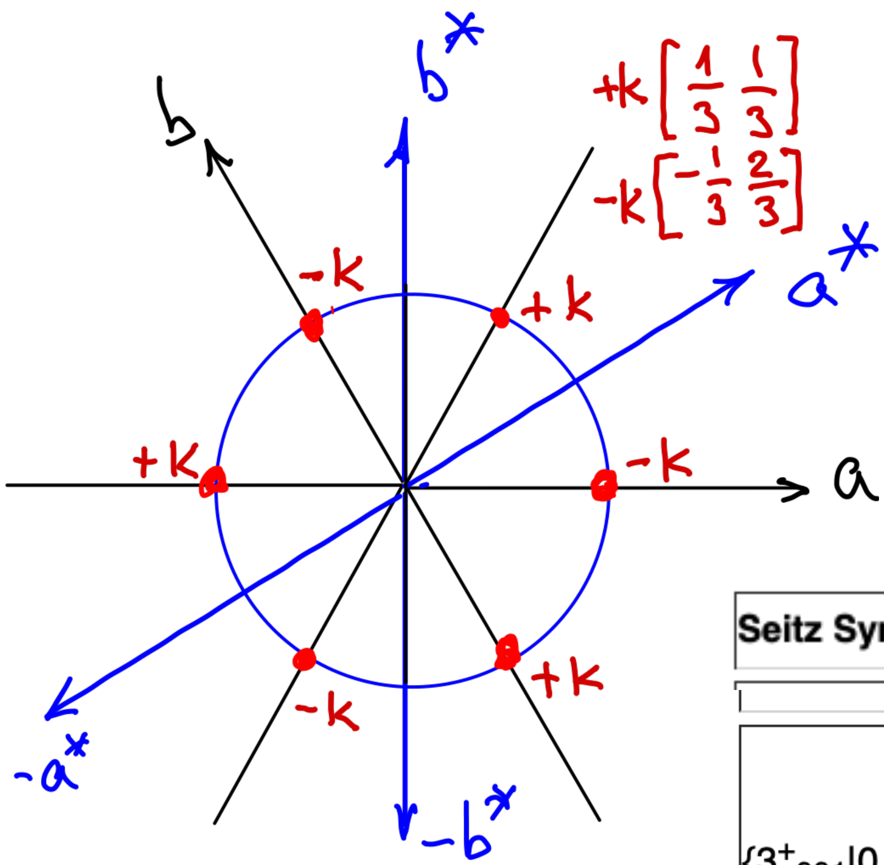

Space group G: 175 P6/m C6h−1
Propagation vector K−point of BZ, k=[1/3,1/3,0]
irreps of the of the little group of propagation vector Gk

	η=1	η=1	η=0	η=0	η=0	η=0
Seitz Symbol	K_1	K_2	K_3	K_4	K_5	K_6
$\{3^+_{001}\|0,0,0\}$	1	1	$e^{i2\pi/3}$	$e^{i2\pi/3}$	$e^{-i2\pi/3}$	$e^{-i2\pi/3}$
$\{3^-_{001}\|0,0,0\}$	1	1	$e^{-i2\pi/3}$	$e^{-i2\pi/3}$	$e^{i2\pi/3}$	$e^{i2\pi/3}$
$\{m_{001}\|0,0,0\}$	1	-1	1	-1	1	-1
$\{\bar{6}^-_{001}\|0,0,0\}$						
$\{\bar{6}^+_{001}\|0,0,0\}$						

representation approach to the magnetic structure in Tb14Ag51

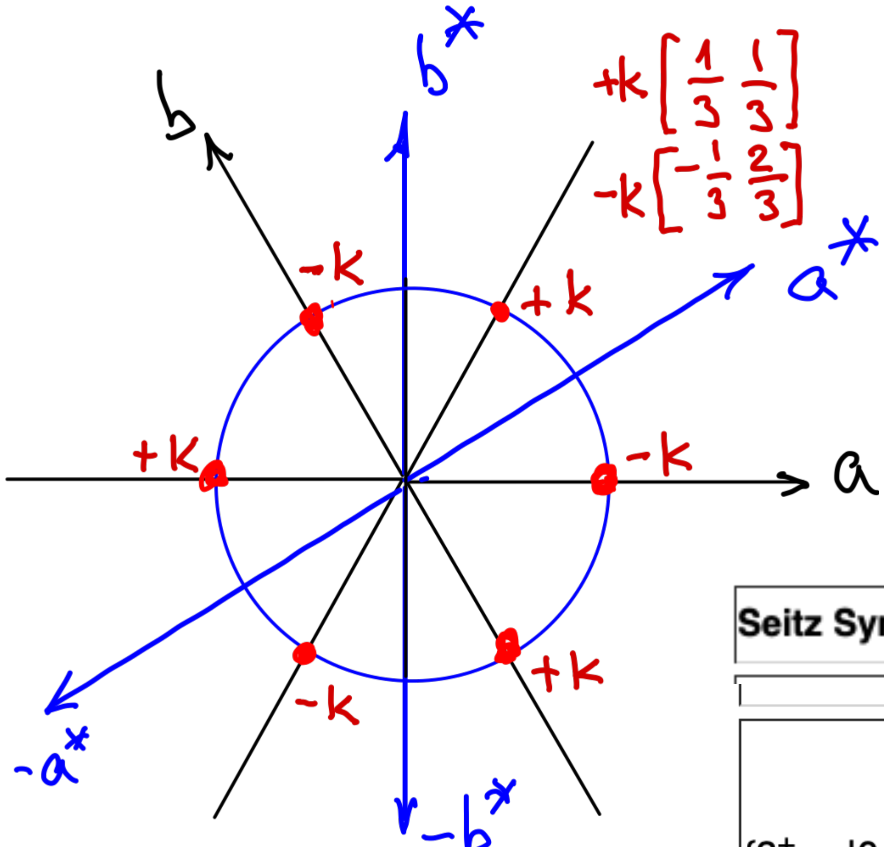

Space group G: 175 P6/m C6h−1
Propagation vector K−point of BZ, k=[1/3,1/3,0]
irreps of the of the little group of propagation vector Gk

	η=1	η=1	η=0	η=0	η=0	η=0
Seitz Symbol	K_1	K_2	K_3	K_4	K_5	K_6
$\{3^+_{001}\|0,0,0\}$	1	1	$e^{i2\pi/3}$	$e^{i2\pi/3}$	$e^{-i2\pi/3}$	$e^{-i2\pi/3}$
$\{3^-_{001}\|0,0,0\}$	1	1	$e^{-i2\pi/3}$	$e^{-i2\pi/3}$	$e^{i2\pi/3}$	$e^{i2\pi/3}$
$\{m_{001}\|0,0,0\}$	1	-1	1	-1	1	-1
$\{\bar{6}^-_{001}\|0,0,0\}$						
$\{\bar{6}^+_{001}\|0,0,0\}$						

representation approach to the magnetic structure in $Tb_{14}Ag_{51}$

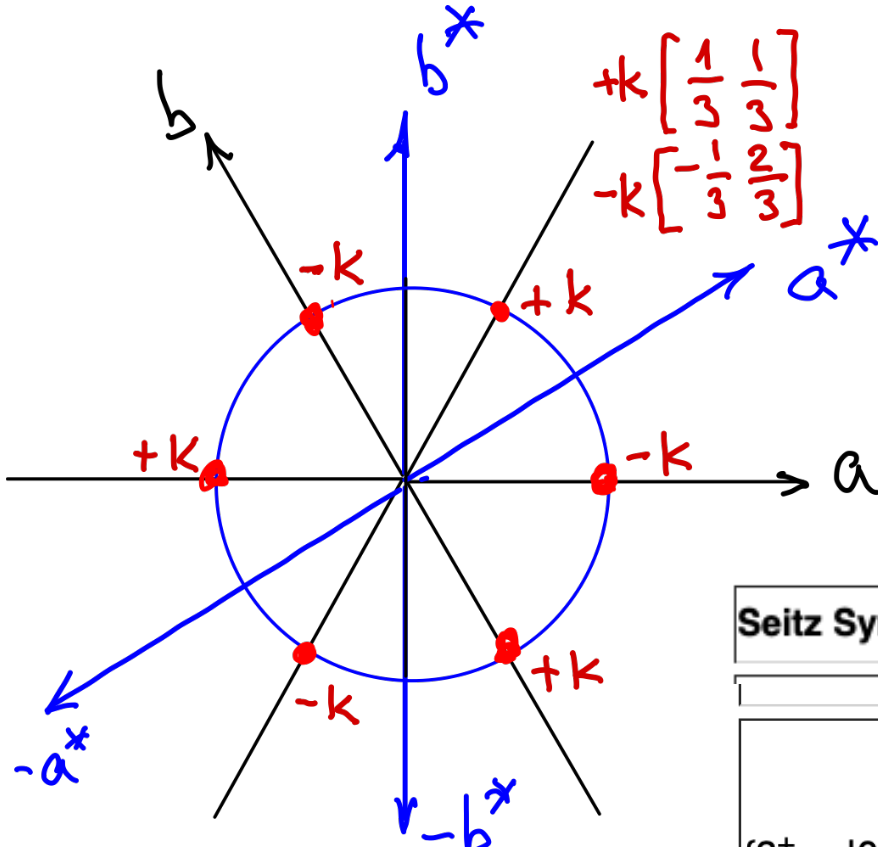

Space group G: 175 P6/m C6h−1
Propagation vector K−point of BZ, k=[1/3,1/3,0]
irreps of the of the little group of propagation vector Gk

	η=1	η=1	η=0	η=0	η=0	η=0
Seitz Symbol	K_1	K_2	K_3	K_4	K_5	K_6
$\{3^+_{001}\|0,0,0\}$	1	1	$e^{i2\pi/3}$	$e^{i2\pi/3}$	$e^{-i2\pi/3}$	$e^{-i2\pi/3}$
$\{3^-_{001}\|0,0,0\}$	1	1	$e^{-i2\pi/3}$	$e^{-i2\pi/3}$	$e^{i2\pi/3}$	$e^{i2\pi/3}$
$\{m_{001}\|0,0,0\}$	1	-1	1	-1	1	-1
$\{\bar{6}^-_{001}\|0,0,0\}$						
$\{\bar{6}^+_{001}\|0,0,0\}$						

complex conjugated c.c
η=0 (type=3)

For complex irrep (η=0) we mix basis functions on the same arm

Hexagonal P6/m space group

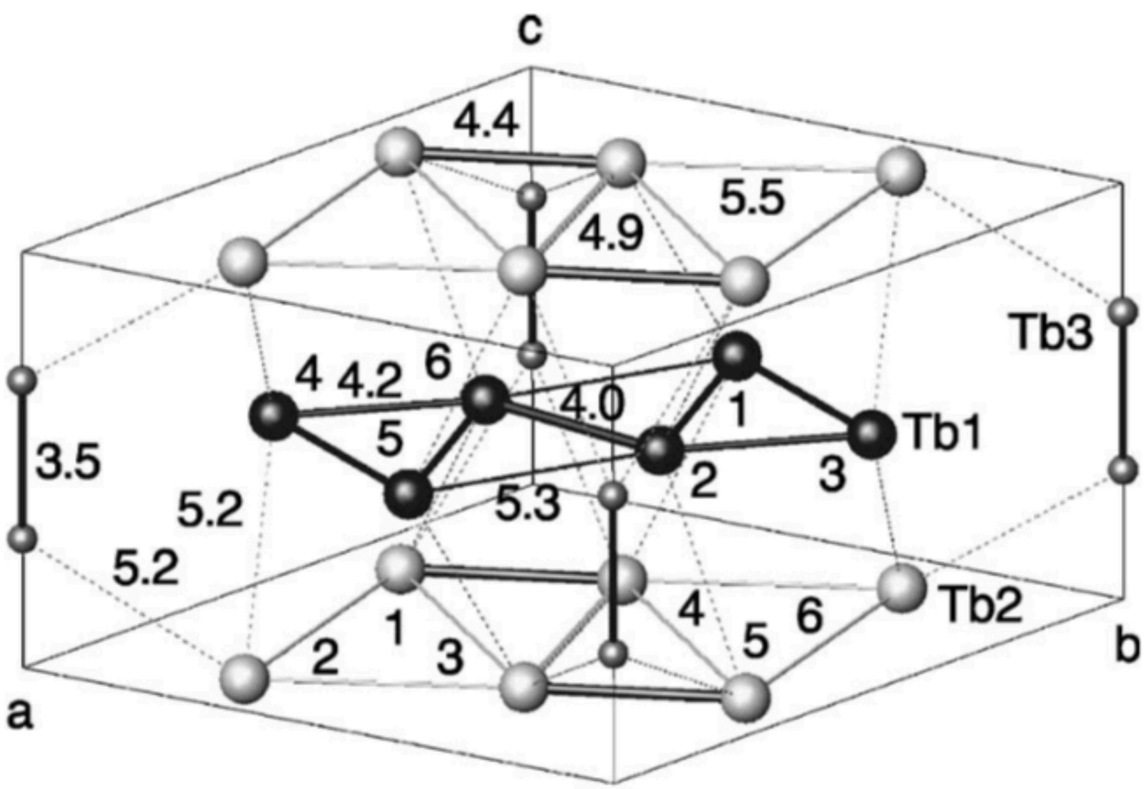

Tb1	6*k*
Tb2	6*j*
Tb3	2*e*

P6/m (175) **k**=[⅓⅓0]

<u>only irrep K4</u> for Tb1

m1 = (mx, my, mz) = C1·(1, exp(iπ/3), 0)

in hex−coordinates is an ideal constant moment **M**(**r**) cycloid

M(**r**) = Re [**m**1·exp(i2π(**k**·**r**))]

(Mx, My, Mz) = C1·(cos(**k**·**r**), cos(**k**·**r**+π/3), 0)

For complex irrep (η=0) we mix basis functions on the same arm

Hexagonal P6/m space group

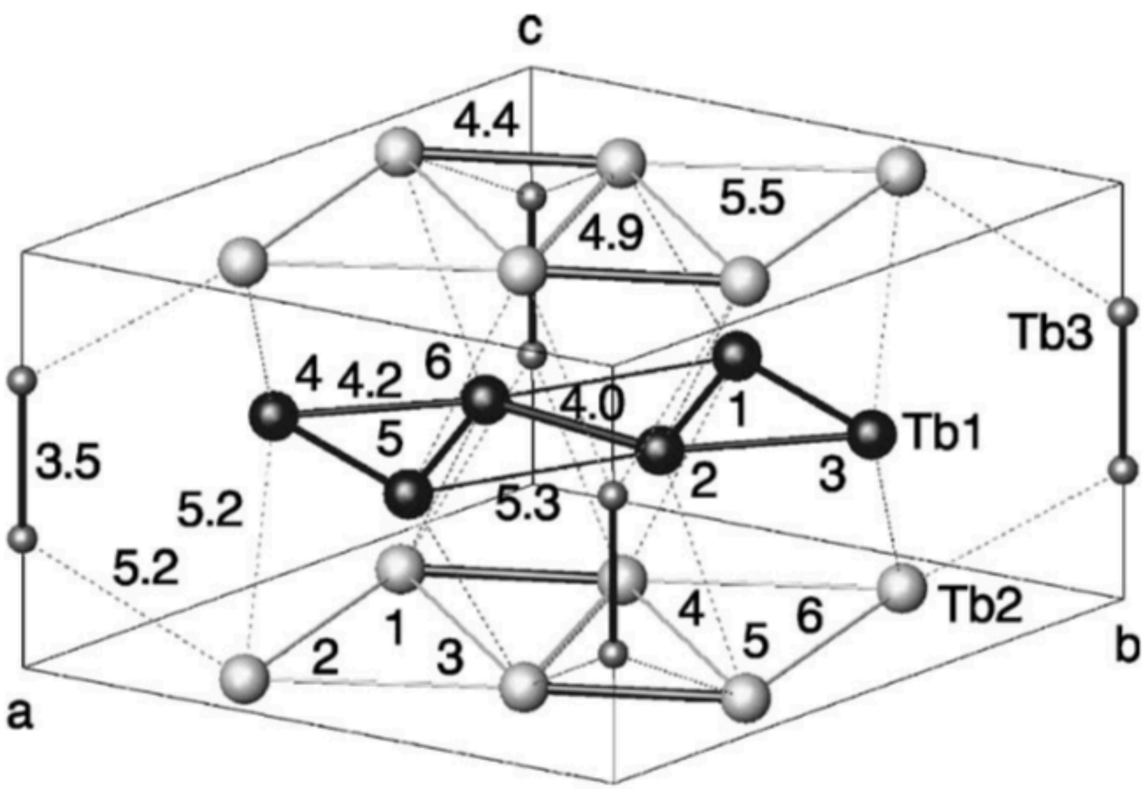

P6/m (175) **k**=[⅓⅓0]

only irrep K4 for Tb1

m1 = (mx, my, mz) = C1·(1, exp(iπ/3), 0)

in hex–coordinates is an ideal constant moment **M**(**r**) cycloid

M(**r**) = Re [**m**1·exp(i2π(**k**·**r**))]

(Mx, My, Mz) = C1·(cos(**k**·**r**), cos(**k**·**r**+π/3), 0)

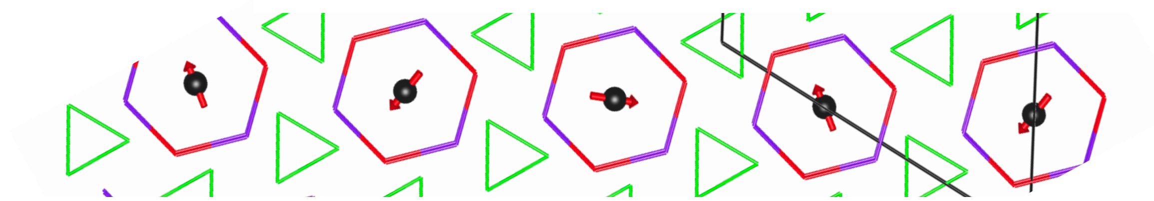

Tb1	6*k*
Tb2	6*j*
Tb3	2*e*

For complex irrep (η=0) we mix basis functions on the same arm

Hexagonal P6/m space group

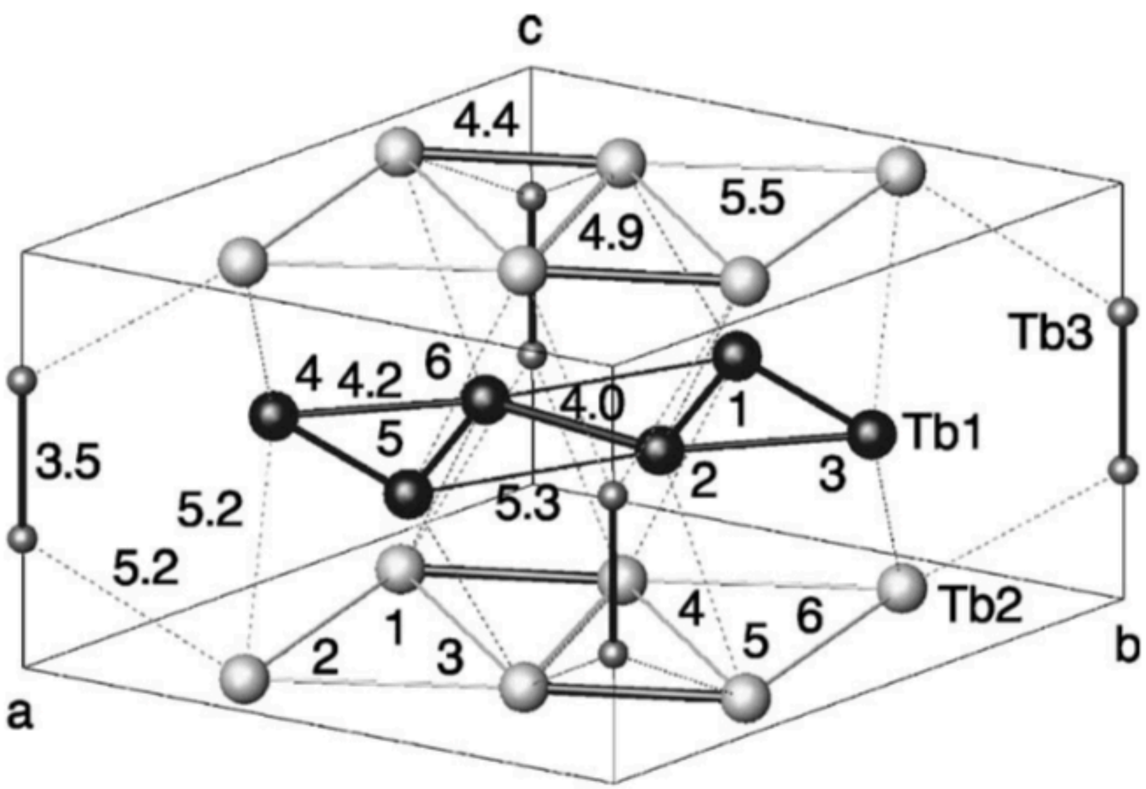

Tb1	6*k*
Tb2	6*j*
Tb3	2*e*

P6/m (175) **k**=[⅓⅓0]

<u>only irrep K4</u> for Tb1

m1 = (mx, my, mz) = C1·(1, exp(iπ/3), 0)

in hex–coordinates is an ideal constant moment **M**(**r**) cycloid

M(**r**) = Re [**m**1·exp(i2π(**k**·**r**))]

(Mx, My, Mz) = C1·(cos(**k**·**r**), cos(**k**·**r**+π/3), 0)

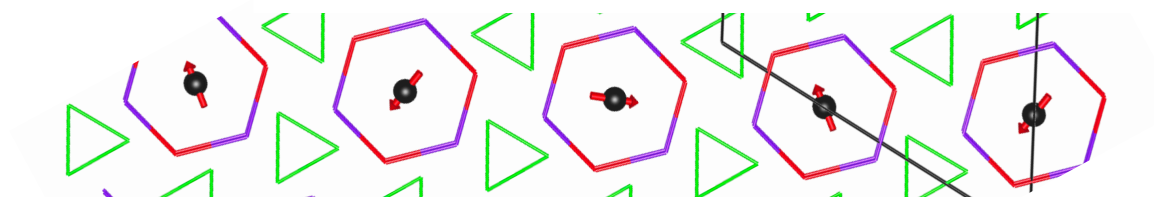

<u>full irrep irrep K4K6</u>

we have to mix two basis functions:

m1 = (mx, my, mz) = C1·(1, exp(+iπ/3), 0)

m2 = (mx, my, mz) = C2·(1, exp(–iπ/3), 0)

BUT…

we do not know how?

One does not need to know technicalities to determine the magnetic structures and one can use advanced software tools as a black box.

Web/computer resources to perform group theory symmetry analysis, in particular magnetic structures.

General tools for representation analysis, Shubnikov groups, 3D+n, and much more...

Two main web sites with a collection of software which applies group theoretical methods to the analysis of phase transitions in crystalline solids.

Harold T. Stokes, Dorian M. Hatch, and Branton J. Campbell

ISODISTORT: ISOTROPY Software Suite http://iso.byu.edu

→ **ISOTROPY Software Suite**
Harold T. Stokes, Dorian M. Hatch, and Branton J. Campbell, Department of Physics and Astronomy, Brigham Young University, Provo, Utah 84606, USA,

BYU BRIGHAM YOUNG UNIVERSITY

M. I. Aroyo, J. M. Perez–Mato, D. Orobengoa, E. Tasci, G. de la Flor, and A. Kirov

Bilbao Crystallographic Server http://www.cryst.ehu.es/

→ **bilbao crystallographic server**

University of the Basque Country
Universidad del País Vasco (UPV)
Euskal Herriko Unibertsitatea (EHU)
eman ta zabal zazu

Four dimensional irrep that generate the magnetic structure in Tb14Ag51

Space group G: 175 P6/m C6h-1
Propagation vector K−point of BZ, k=[1/3,1/3,0]

Pair of conjugated
non−equivalent irreps for
little group G_k IR

		K4	K6
$\begin{pmatrix} 0 & -1 & 0 & 0 \\ 1 & -1 & 0 & 0 \\ 0 & 0 & 1 & 0 \end{pmatrix}$	$\{3^{+}_{001}\|0,0,0\}$	$e^{i2\pi/3}$	$e^{-i2\pi/3}$
$\begin{pmatrix} -1 & 1 & 0 & 0 \\ -1 & 0 & 0 & 0 \\ 0 & 0 & 1 & 0 \end{pmatrix}$	$\{3^{-}_{001}\|0,0,0\}$	$e^{-i2\pi/3}$	$e^{i2\pi/3}$
$\begin{pmatrix} -1 & 0 & 0 & 0 \\ 0 & -1 & 0 & 0 \\ 0 & 0 & 1 & 0 \end{pmatrix}$	$\{2_{001}\|0,0,0\}$		

Four dimensional irrep that generate the magnetic structure in Tb14Ag51

Space group G: 175 P6/m C6h-1
Propagation vector K−point of BZ, k=[1/3,1/3,0]

		Pair of conjugated **non−equivalent** irreps for little group G_k IR: K4	K6	G IR: K4
$\begin{pmatrix} 0 & -1 & 0 & 0 \\ 1 & -1 & 0 & 0 \\ 0 & 0 & 1 & 0 \end{pmatrix}$	$\{3^+_{001}\|0,0,0\}$	$e^{i2\pi/3}$	$e^{-i2\pi/3}$	$\begin{pmatrix} e^{i2\pi/3} & 0 \\ 0 & e^{i2\pi/3} \end{pmatrix}$
$\begin{pmatrix} -1 & 1 & 0 & 0 \\ -1 & 0 & 0 & 0 \\ 0 & 0 & 1 & 0 \end{pmatrix}$	$\{3^-_{001}\|0,0,0\}$	$e^{-i2\pi/3}$	$e^{i2\pi/3}$	$\begin{pmatrix} e^{-i2\pi/3} & 0 \\ 0 & e^{-i2\pi/3} \end{pmatrix}$
$\begin{pmatrix} -1 & 0 & 0 & 0 \\ 0 & -1 & 0 & 0 \\ 0 & 0 & 1 & 0 \end{pmatrix}$	$\{2_{001}\|0,0,0\}$			$\begin{pmatrix} 0 & -1 \\ -1 & 0 \end{pmatrix}$

Four dimensional irrep that generate the magnetic structure in Tb14Ag51

Space group G: 175 P6/m C6h-1
Propagation vector K−point of BZ, k=[1/3,1/3,0]

		Pair of conjugated **non−equivalent** irreps for little group G_k IR		G IR	mK4K6 PIR=IR
		K4	K6	K4	
$\begin{pmatrix} 0 & -1 & 0 & 0 \\ 1 & -1 & 0 & 0 \\ 0 & 0 & 1 & 0 \end{pmatrix}$	$\{3^{+}_{001}\|0,0,0\}$	$e^{i2\pi/3}$	$e^{-i2\pi/3}$	$\begin{pmatrix} e^{i2\pi/3} & 0 \\ 0 & e^{i2\pi/3} \end{pmatrix}$	$\begin{pmatrix} -1/2 & 0 & \sqrt{3}/2 & 0 \\ 0 & -1/2 & 0 & -\sqrt{3}/2 \\ -\sqrt{3}/2 & 0 & -1/2 & 0 \\ 0 & \sqrt{3}/2 & 0 & -1/2 \end{pmatrix}$
$\begin{pmatrix} -1 & 1 & 0 & 0 \\ -1 & 0 & 0 & 0 \\ 0 & 0 & 1 & 0 \end{pmatrix}$	$\{3^{-}_{001}\|0,0,0\}$	$e^{-i2\pi/3}$	$e^{i2\pi/3}$	$\begin{pmatrix} e^{-i2\pi/3} & 0 \\ 0 & e^{-i2\pi/3} \end{pmatrix}$	$\begin{pmatrix} -1/2 & 0 & -\sqrt{3}/2 & 0 \\ 0 & -1/2 & 0 & \sqrt{3}/2 \\ \sqrt{3}/2 & 0 & -1/2 & 0 \\ 0 & -\sqrt{3}/2 & 0 & -1/2 \end{pmatrix}$
$\begin{pmatrix} -1 & 0 & 0 & 0 \\ 0 & -1 & 0 & 0 \\ 0 & 0 & 1 & 0 \end{pmatrix}$	$\{2_{001}\|0,0,0\}$			$\begin{pmatrix} 0 & -1 \\ -1 & 0 \end{pmatrix}$	$\begin{pmatrix} 0 & -\sqrt{3}/2 & 0 & -1/2 \\ -\sqrt{3}/2 & 0 & -1/2 & 0 \\ 0 & -1/2 & 0 & \sqrt{3}/2 \\ -1/2 & 0 & \sqrt{3}/2 & 0 \end{pmatrix}$

Four dimensional irrep that generate the magnetic structure in Tb14Ag51

Space group G: 175 P6/m C6h-1
Propagation vector K−point of BZ, k=[1/3,1/3,0]

		Pair of conjugated **non−equivalent** irreps for little group G_k IR		G IR	mK4K6 PIR=IR	Order Parameter direction OPD
		K4	K6	K4		
$\begin{pmatrix} 0 & -1 & 0 & 0 \\ 1 & -1 & 0 & 0 \\ 0 & 0 & 1 & 0 \end{pmatrix}$	$\{3^{+}_{001}\|0,0,0\}$	$e^{i2\pi/3}$	$e^{-i2\pi/3}$	$\begin{pmatrix} e^{i2\pi/3} & 0 \\ 0 & e^{i2\pi/3} \end{pmatrix}$	$\begin{pmatrix} -1/2 & 0 & \sqrt{3}/2 & 0 \\ 0 & -1/2 & 0 & -\sqrt{3}/2 \\ -\sqrt{3}/2 & 0 & -1/2 & 0 \\ 0 & \sqrt{3}/2 & 0 & -1/2 \end{pmatrix}$	$\begin{pmatrix} a \\ b \\ c \\ d \end{pmatrix}$
$\begin{pmatrix} -1 & 1 & 0 & 0 \\ -1 & 0 & 0 & 0 \\ 0 & 0 & 1 & 0 \end{pmatrix}$	$\{3^{-}_{001}\|0,0,0\}$	$e^{-i2\pi/3}$	$e^{i2\pi/3}$	$\begin{pmatrix} e^{-i2\pi/3} & 0 \\ 0 & e^{-i2\pi/3} \end{pmatrix}$	$\begin{pmatrix} -1/2 & 0 & -\sqrt{3}/2 & 0 \\ 0 & -1/2 & 0 & \sqrt{3}/2 \\ \sqrt{3}/2 & 0 & -1/2 & 0 \\ 0 & -\sqrt{3}/2 & 0 & -1/2 \end{pmatrix}$	
$\begin{pmatrix} -1 & 0 & 0 & 0 \\ 0 & -1 & 0 & 0 \\ 0 & 0 & 1 & 0 \end{pmatrix}$	$\{2_{001}\|0,0,0\}$			$\begin{pmatrix} 0 & -1 \\ -1 & 0 \end{pmatrix}$	$\begin{pmatrix} 0 & -\sqrt{3}/2 & 0 & -1/2 \\ -\sqrt{3}/2 & 0 & -1/2 & 0 \\ 0 & -1/2 & 0 & \sqrt{3}/2 \\ -1/2 & 0 & \sqrt{3}/2 & 0 \end{pmatrix}$	

This OPD vector should stay invariant under action some of some of the matrices. Those group elements, whose matrices leave the vector invariant form isotropy magnetic subgroup.

Four dimensional irrep that generate the magnetic structure in Tb14Ag51

Space group G: 175 P6/m C6h-1
Propagation vector K−point of BZ, k=[1/3,1/3,0]

		Pair of conjugated **non−equivalent** irreps for little group G_k IR: K4	K6	G IR: K4	mK4K6 PIR=IR	Order Parameter direction OPD
$\begin{pmatrix} 0 & -1 & 0 & 0 \\ 1 & -1 & 0 & 0 \\ 0 & 0 & 1 & 0 \end{pmatrix}$	$\{3^+_{001}\|0,0,0\}$	$e^{i2\pi/3}$	$e^{-i2\pi/3}$	$\begin{pmatrix} e^{i2\pi/3} & 0 \\ 0 & e^{i2\pi/3} \end{pmatrix}$	$\begin{pmatrix} -1/2 & 0 & \sqrt{3}/2 & 0 \\ 0 & -1/2 & 0 & -\sqrt{3}/2 \\ -\sqrt{3}/2 & 0 & -1/2 & 0 \\ 0 & \sqrt{3}/2 & 0 & -1/2 \end{pmatrix}$	$\begin{pmatrix} a \\ b \\ c \\ d \end{pmatrix}$ $\begin{pmatrix} a \\ 0 \\ b \\ 0 \end{pmatrix}$
$\begin{pmatrix} -1 & 1 & 0 & 0 \\ -1 & 0 & 0 & 0 \\ 0 & 0 & 1 & 0 \end{pmatrix}$	$\{3^-_{001}\|0,0,0\}$	$e^{-i2\pi/3}$	$e^{i2\pi/3}$	$\begin{pmatrix} e^{-i2\pi/3} & 0 \\ 0 & e^{-i2\pi/3} \end{pmatrix}$	$\begin{pmatrix} -1/2 & 0 & -\sqrt{3}/2 & 0 \\ 0 & -1/2 & 0 & \sqrt{3}/2 \\ \sqrt{3}/2 & 0 & -1/2 & 0 \\ 0 & -\sqrt{3}/2 & 0 & -1/2 \end{pmatrix}$	
$\begin{pmatrix} -1 & 0 & 0 & 0 \\ 0 & -1 & 0 & 0 \\ 0 & 0 & 1 & 0 \end{pmatrix}$	$\{2_{001}\|0,0,0\}$			$\begin{pmatrix} 0 & -1 \\ -1 & 0 \end{pmatrix}$	$\begin{pmatrix} 0 & -\sqrt{3}/2 & 0 & -1/2 \\ -\sqrt{3}/2 & 0 & -1/2 & 0 \\ 0 & -1/2 & 0 & \sqrt{3}/2 \\ -1/2 & 0 & \sqrt{3}/2 & 0 \end{pmatrix}$	

This OPD vector should stay invariant under action some of some of the matrices. Those group elements, whose matrices leave the vector invariant form isotropy magnetic subgroup.

Possible alternative magnetic symmetries if the spin arrangement transforms according to the four-dimensional physically irreducible representation mK4K6.

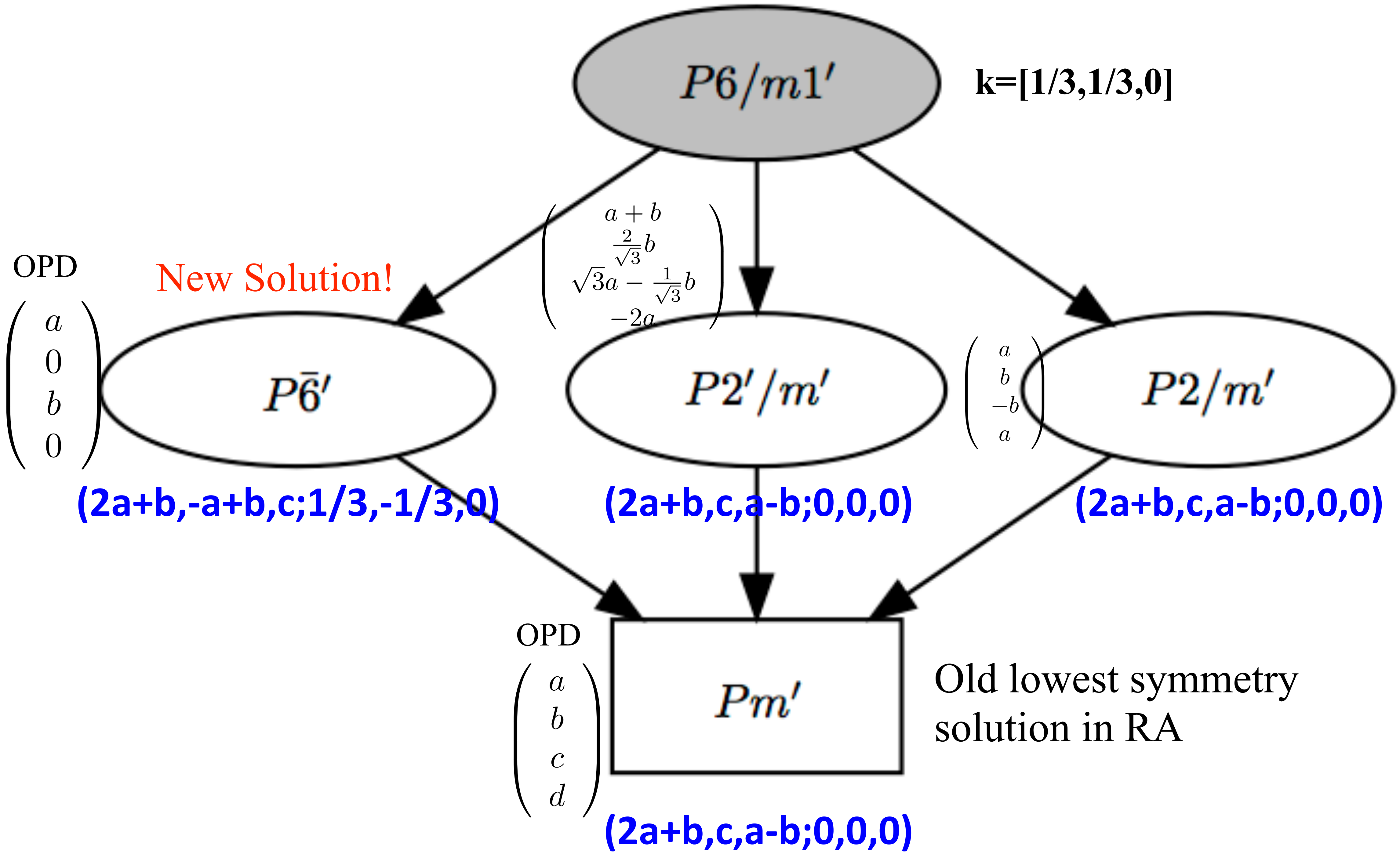

Possible alternative magnetic symmetries if the spin arrangement transforms according to the four-dimensional physically irreducible representation mK4K6.

1. Restrict the symmetry to hex.
2. In addition to modes of **k=[1/3,1/3,0]** allows modes with **k_0=[0,0,0]**, which is 3rd harmonic of k

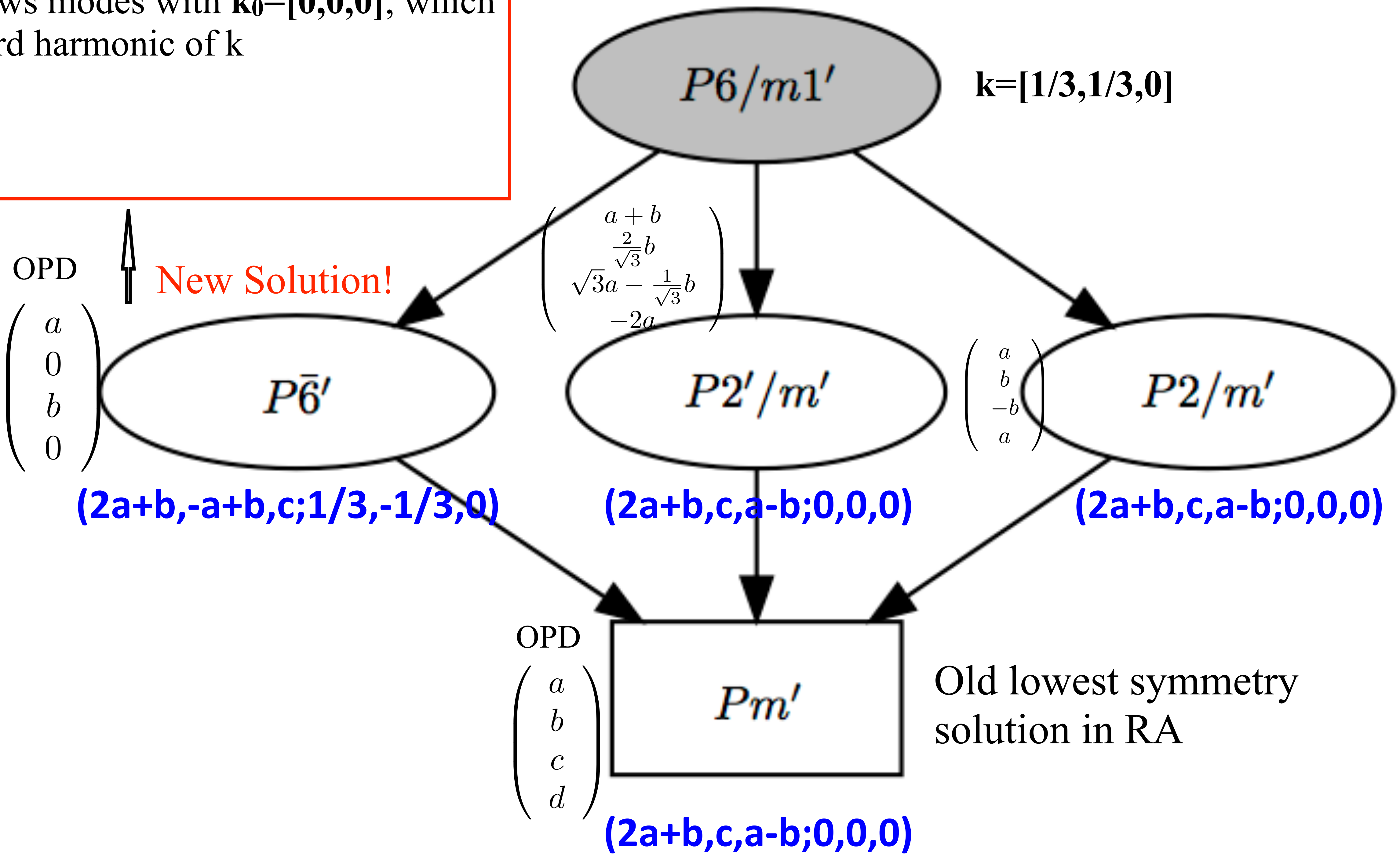

Possible alternative magnetic symmetries if the spin arrangement transforms according to the four-dimensional physically irreducible representation mK4K6.

1. Restrict the symmetry to hex.
2. In addition to modes of **k=[1/3,1/3,0]** allows modes with **k_0=[0,0,0]**, which is 3rd harmonic of k

One mode mGM1- for Tb3 with **M** || c-axis, and modes of mGM1- and mGM2+ with **M** ⊥ c-axis for Tb1 and Tb2.

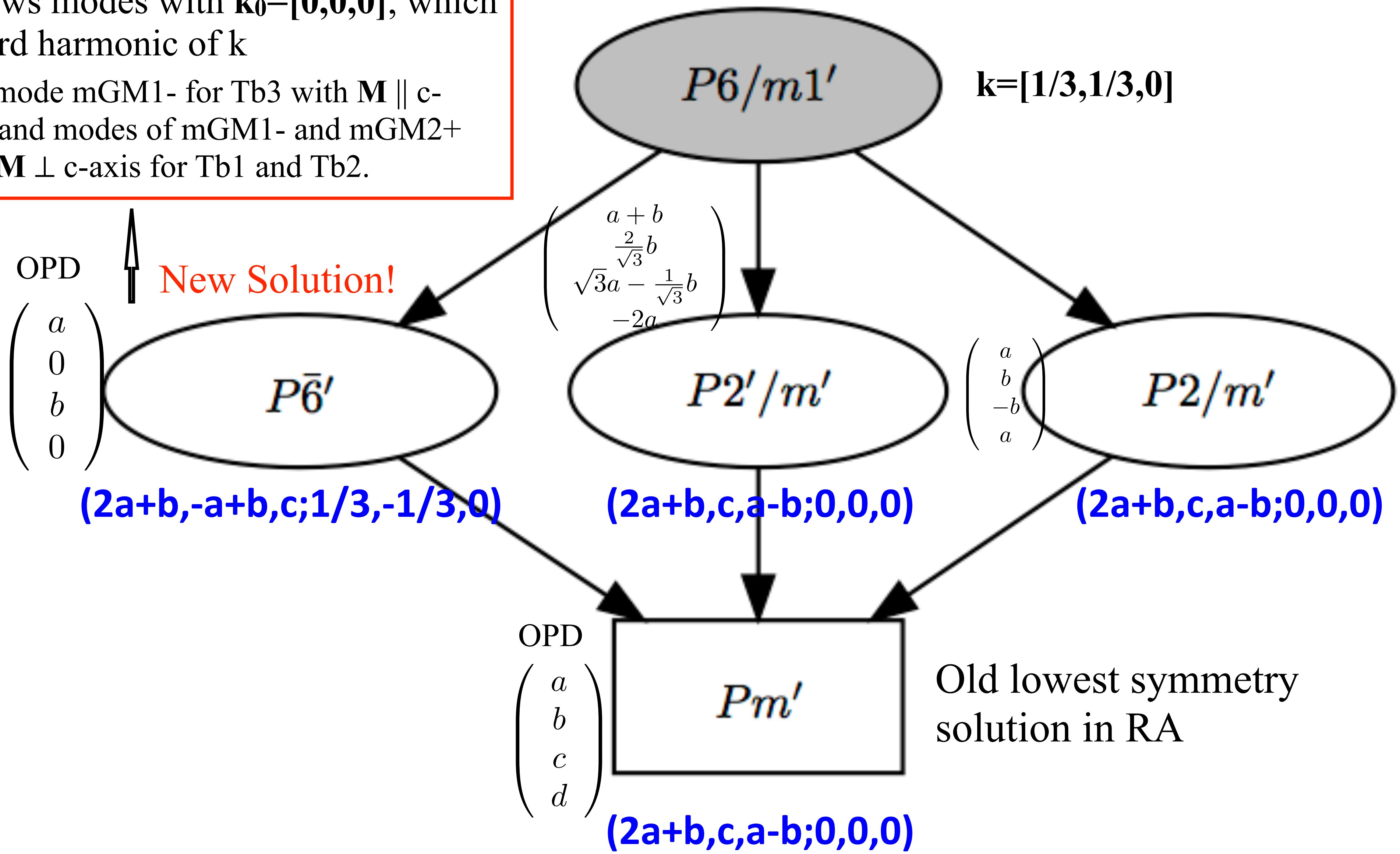

A note on the relations between irreps and magnetic symmetry

irrep: only mK4mK6 k=[1/3,1/3,0] as a primary mode, no k_0=[0,0,0]-contribution. It is possible to introduce 3rd harmonics k_0 = 3k, but respective irreps need to be selected, which is not trivial without symmetry.

magnetic symmetry MSG: the modes of primary irrep k and and the secondary ones k_0 are 'entangled' and add up.

```
TB1_1 -0.88942 -2.72166 0.00000 Mx,My,0
TB1_2  1.04243  4.18925 0.00000 Mx,My,0
TB1_3 -0.15301 -1.46760 0.00000 Mx,My,0
…
```

An artificial example: if the irrep is pseudo-real (−1) the number of alternative symmetries is smaller than for complex one.

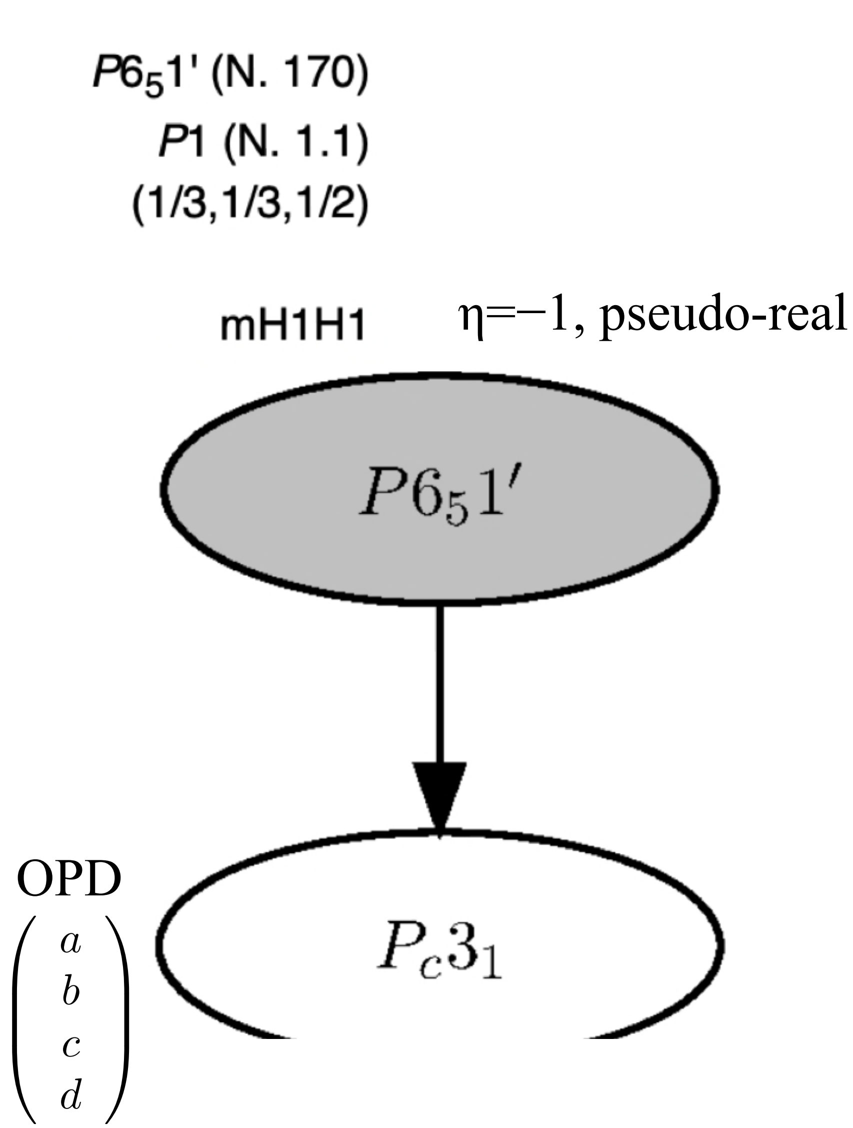

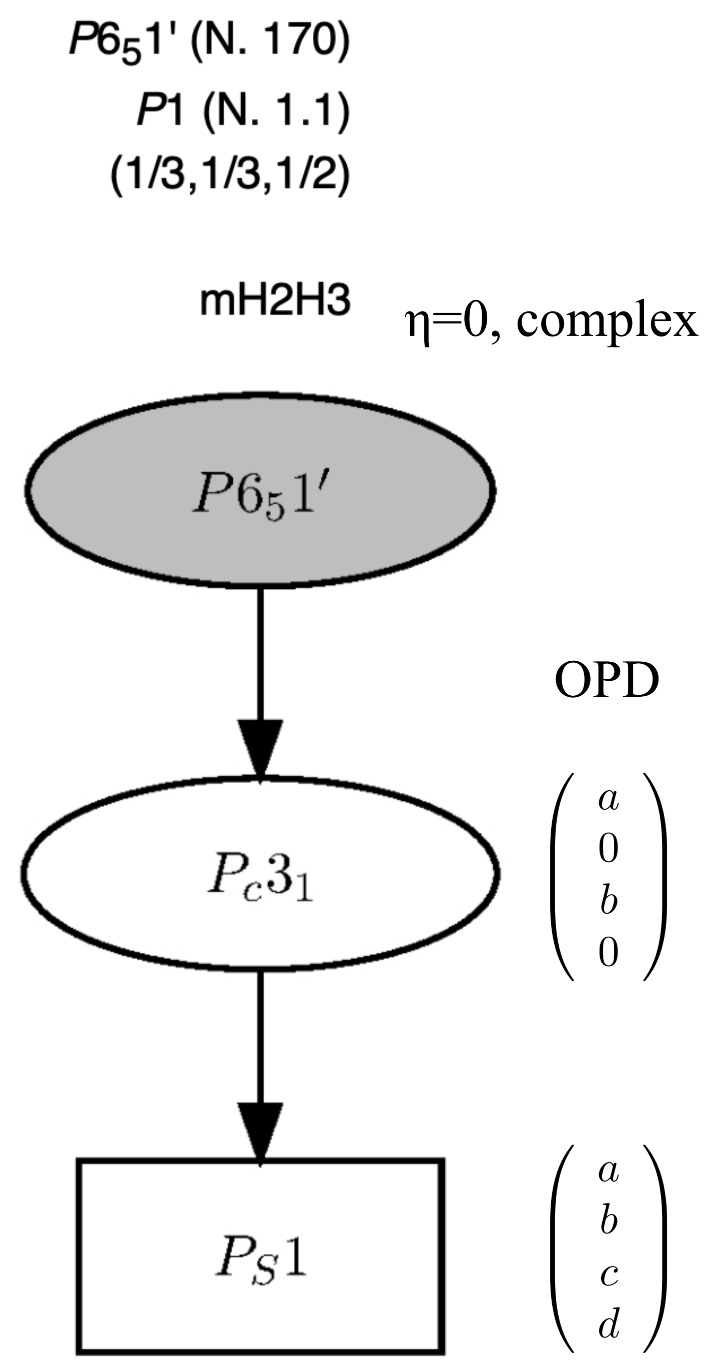

Neutron diffraction experiments

Old solution (2006): only k-point, but Pm'

Difference neutron powder diffraction pattern between at T = 1.5 and 30 K.

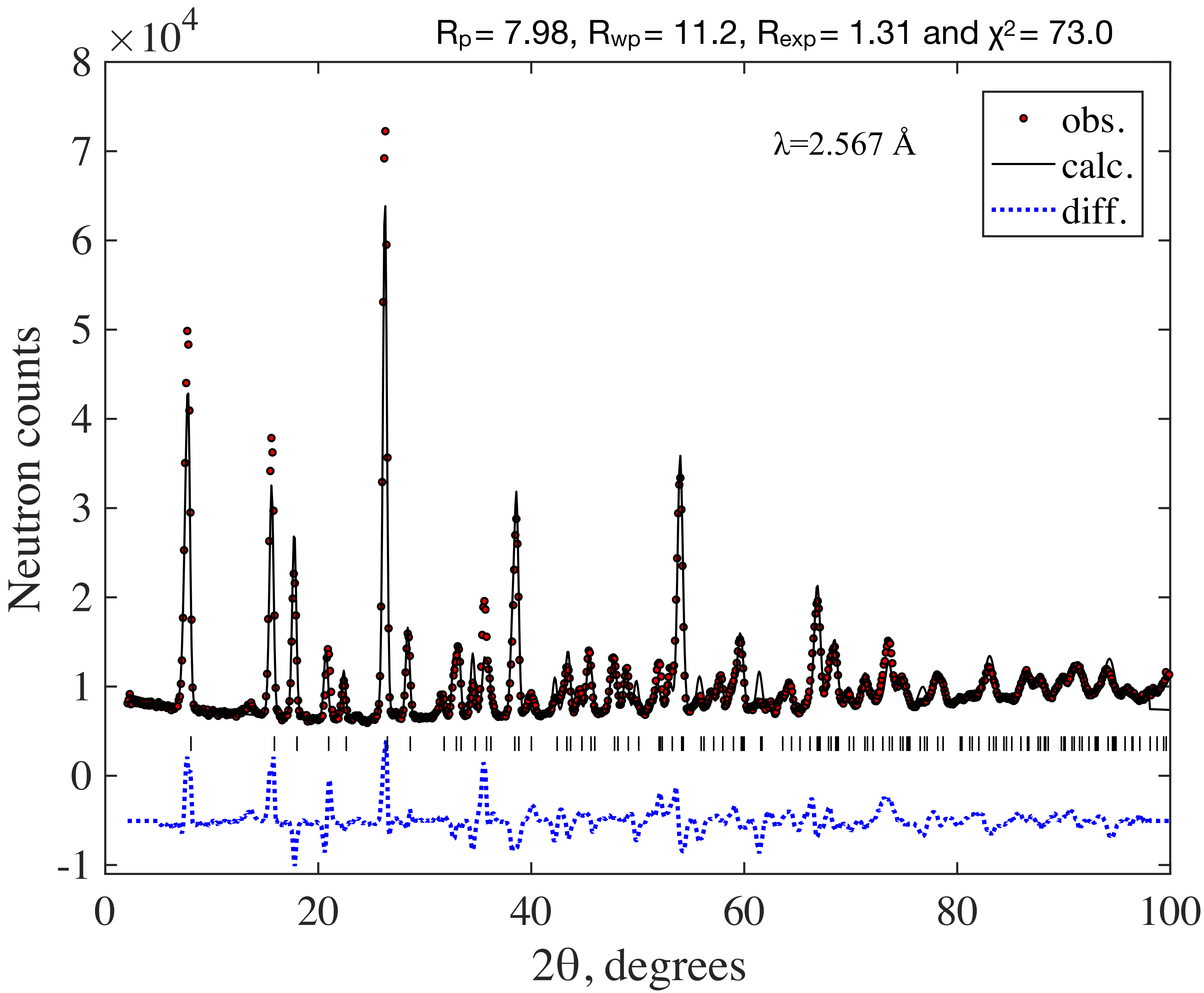

Old fit (only k-point irrep but arbitrary irrep mix)

Neutron powder diffraction pattern measured at T = 1.5K with wavelength 2.567 Å.

Blue – magnetic contribution.

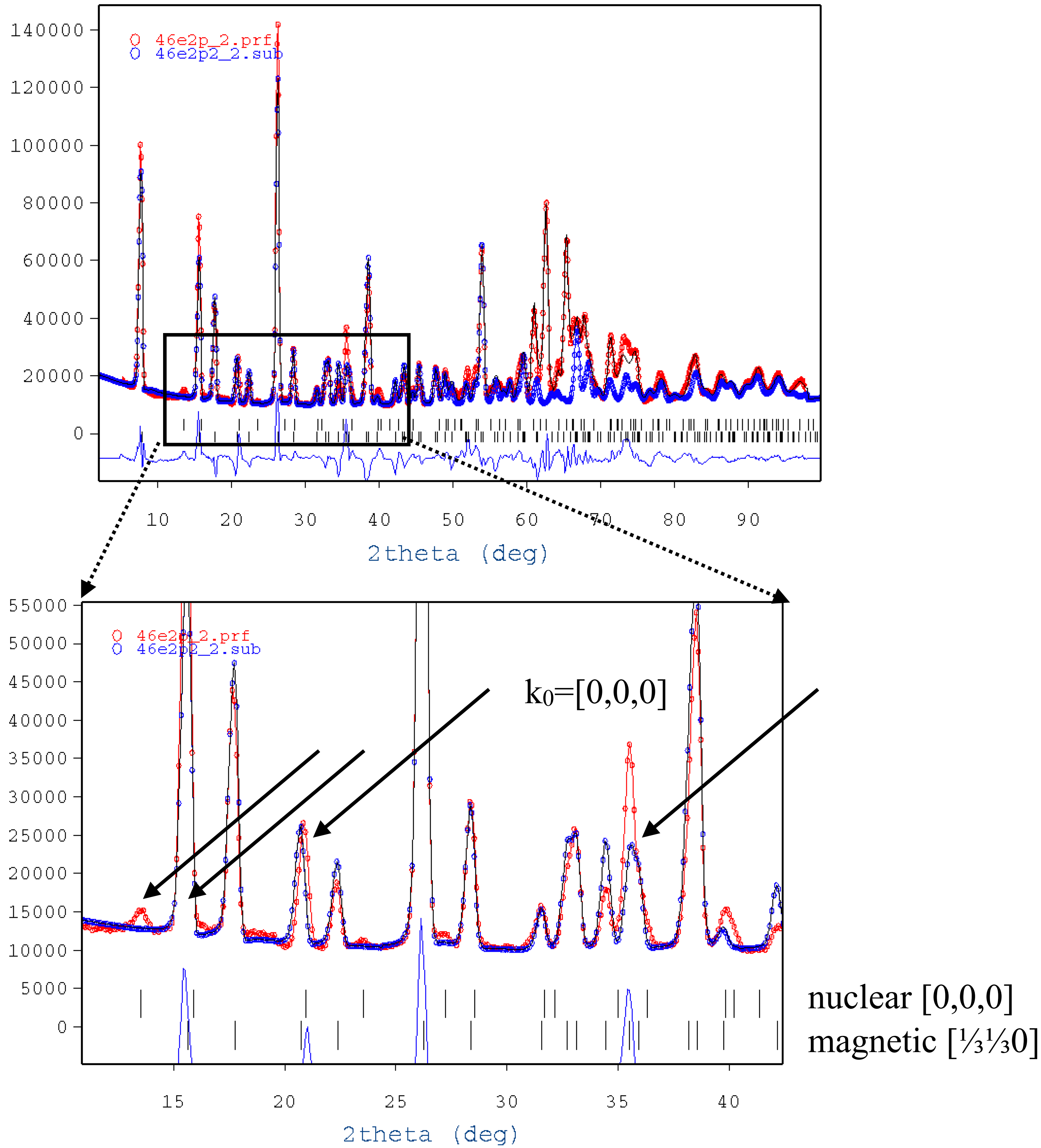

Le Bail vs. new model

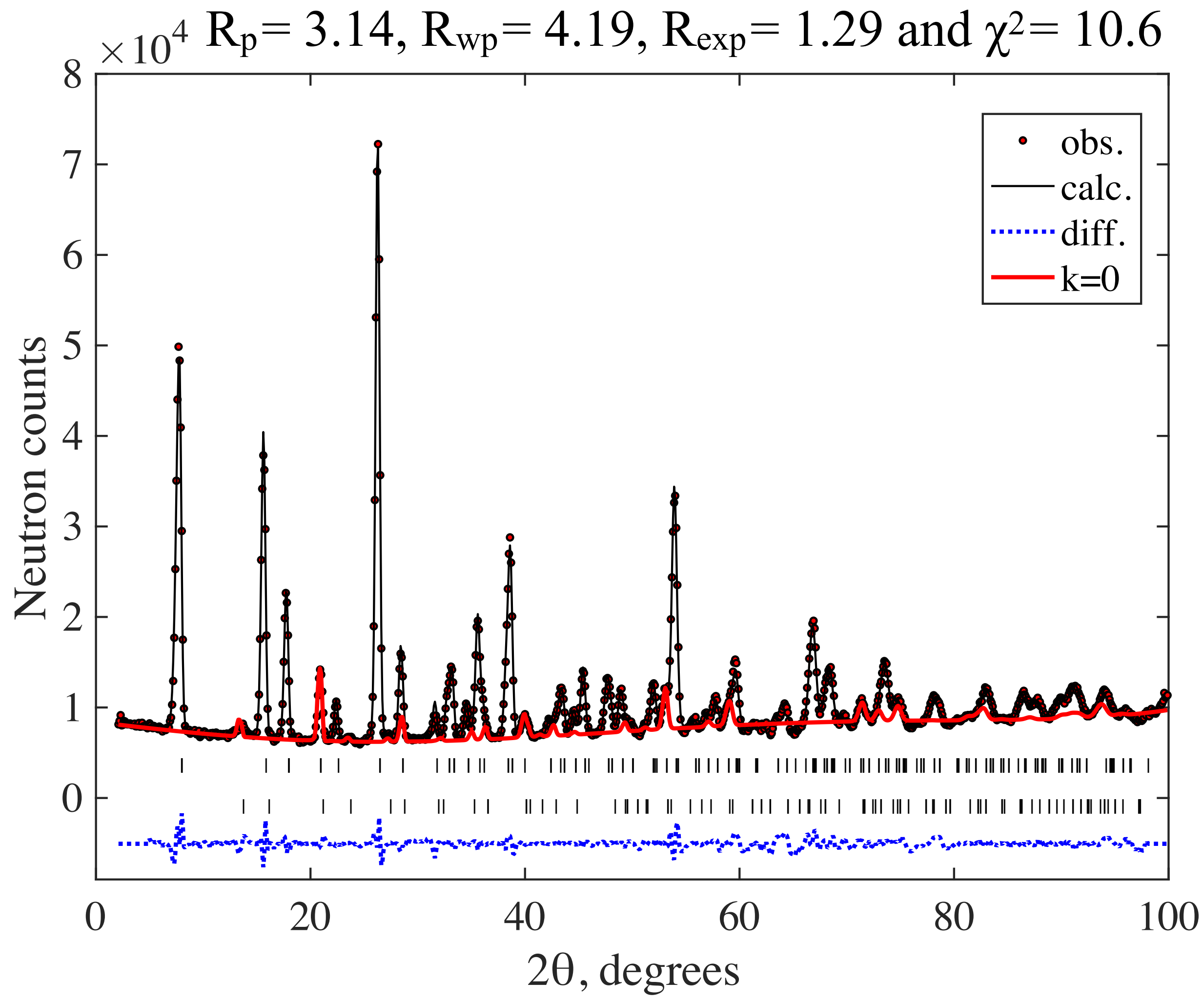

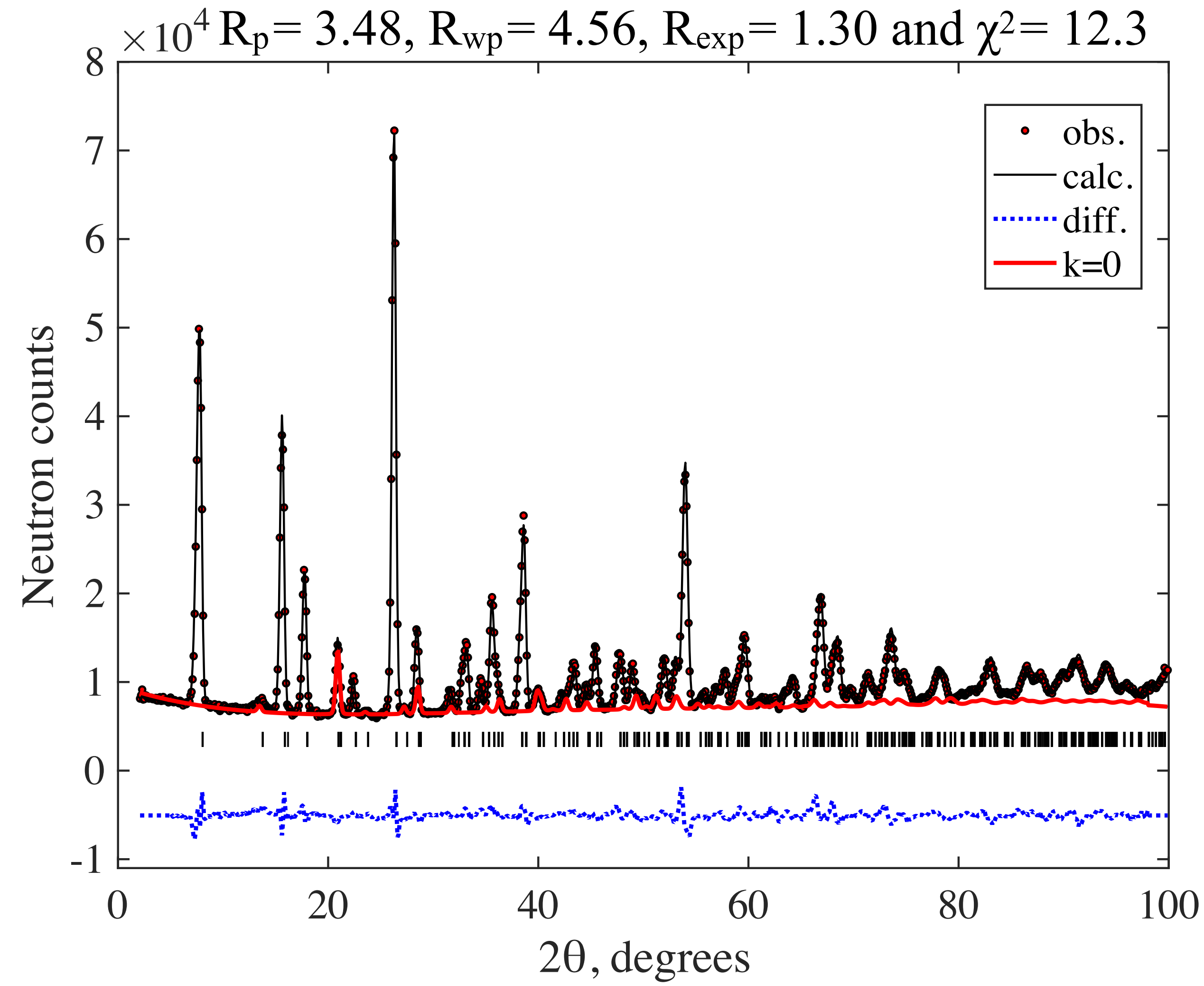

P-6'

27 parameters, which reduce to 15 assuming constant moment

Tb1	6*k* →	6 sites 3k
Tb2	6*j* →	6 sites 3j
Tb3	2*e* →	1 site 6l

78 if only irreps without symmetry

P-6’ AFM structure of Tb14Ag51

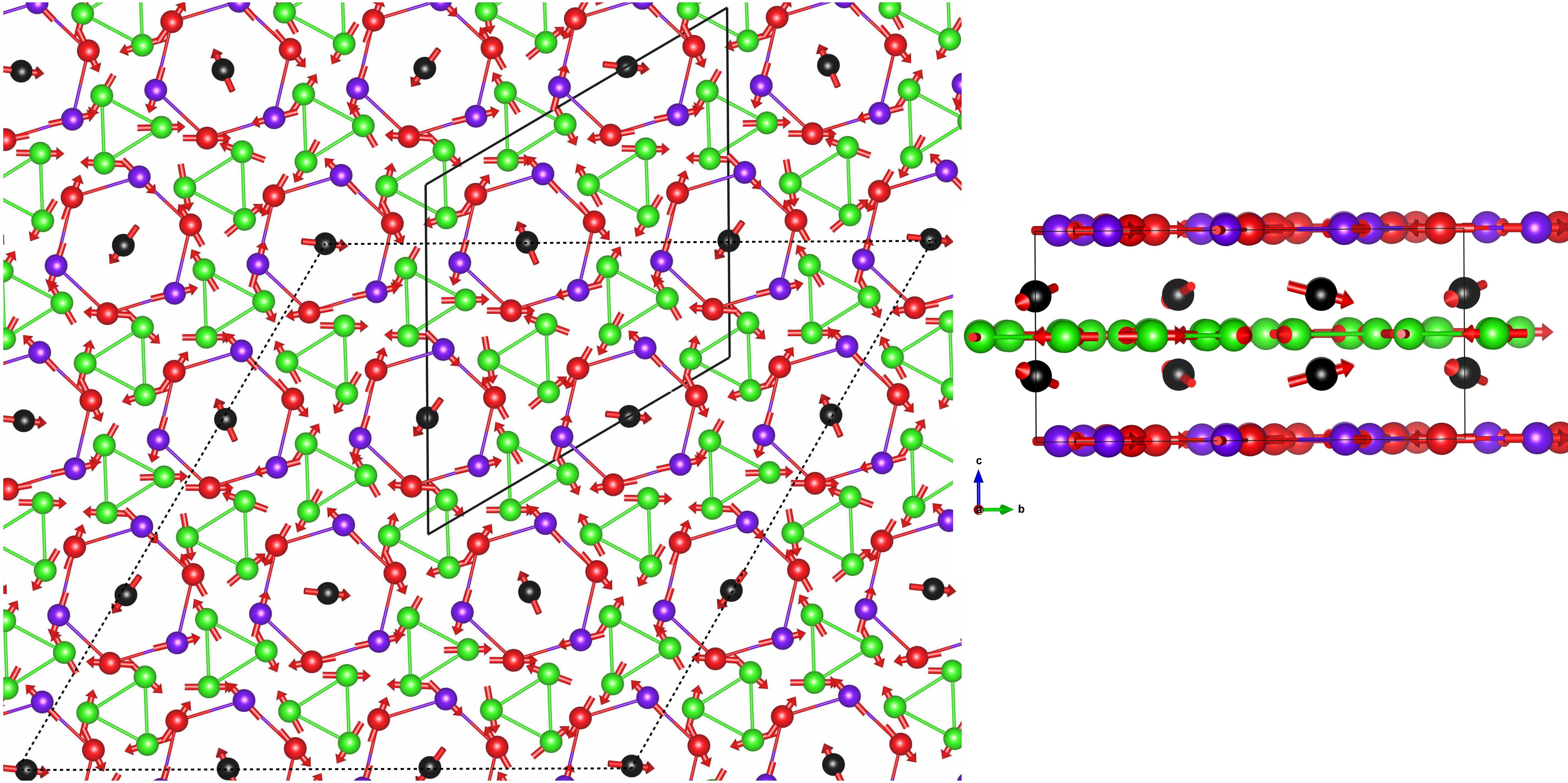

View of the magnetic structure (a) in projection on the xy plane and (b) along the a axis corresponding to the refined model with P6’ symmetry. The unit cell is indicated by a black solid line. The dotted line shows a 3a x 3b supercell of the parent space group P6/m. Tb1 atoms are in green forming the triangles and Tb3 atoms are in black at the centres of hexagons. Tb2a_1, Tb2a_2 and Tb2a_3 are in red, and the remaining three atoms derived from the Tb2 site are in blue.

Decomposition of P-6' AFM structure of Tb14Ag5 into harmonics

It is remarkable that the two modes separately do not maintain a common moment magnitude for all atoms, and this is only attained through the combination of the two contributions

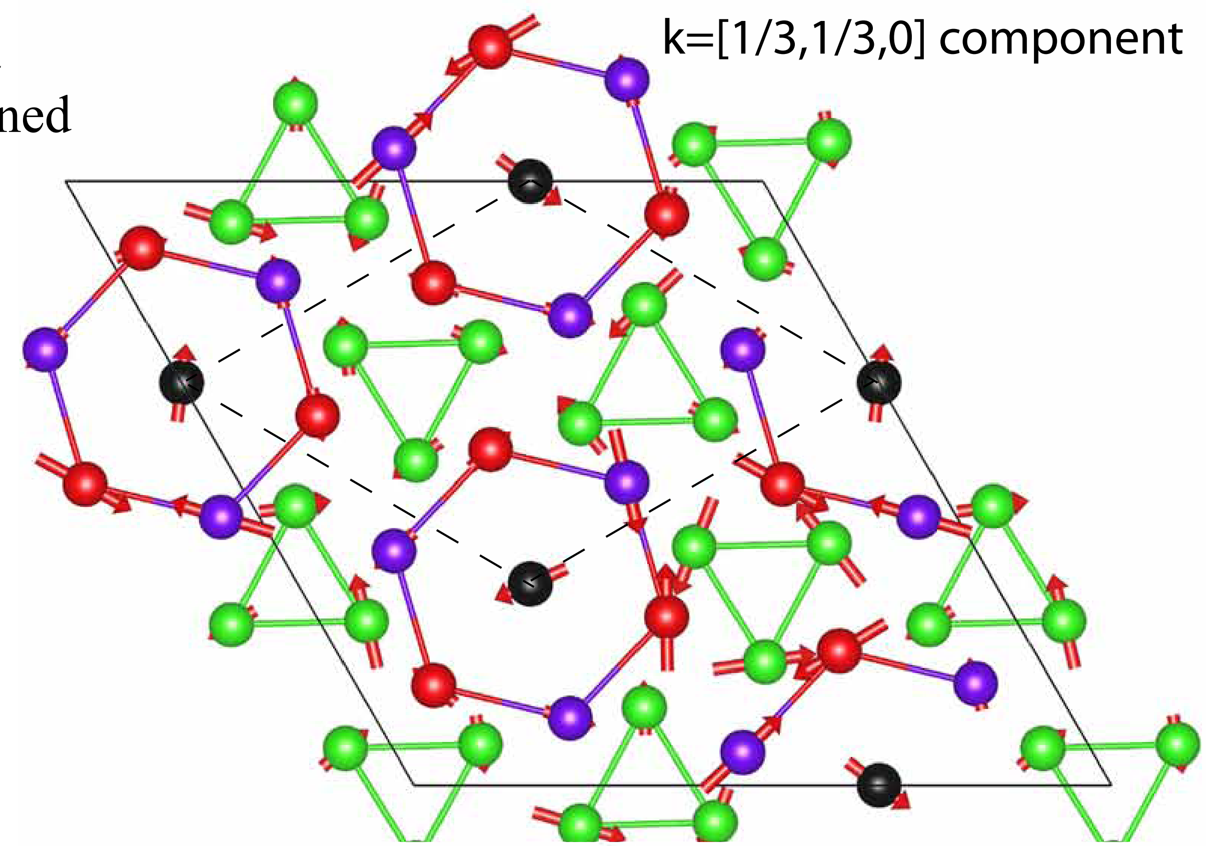

k=[1/3,1/3,0] component

P-6' structure

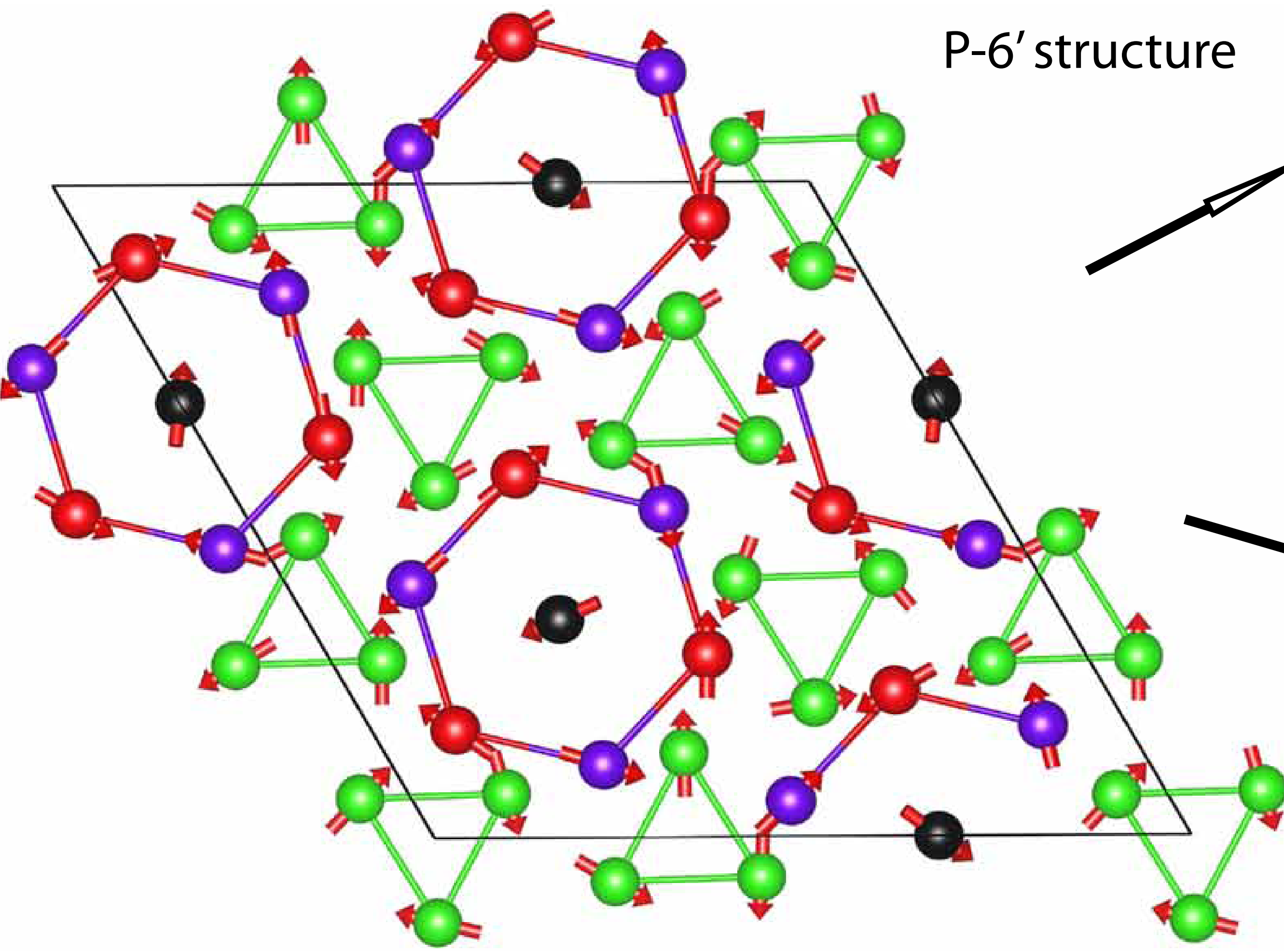

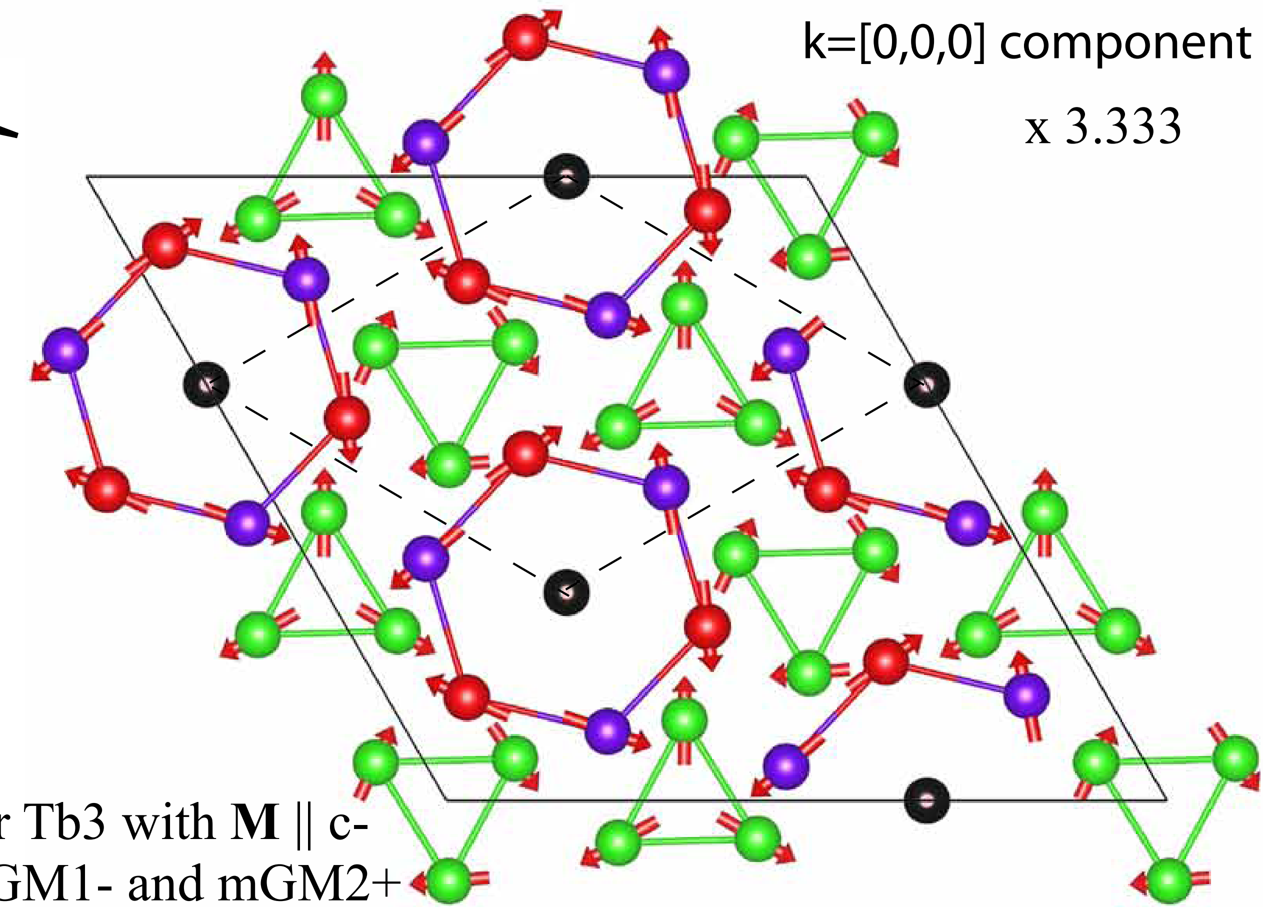

k=[0,0,0] component

x 3.333

One mode mGM1- for Tb3 with **M** || c-axis, and modes of mGM1- and mGM2+ with **M** ⊥ c-axis for Tb1 and Tb2.

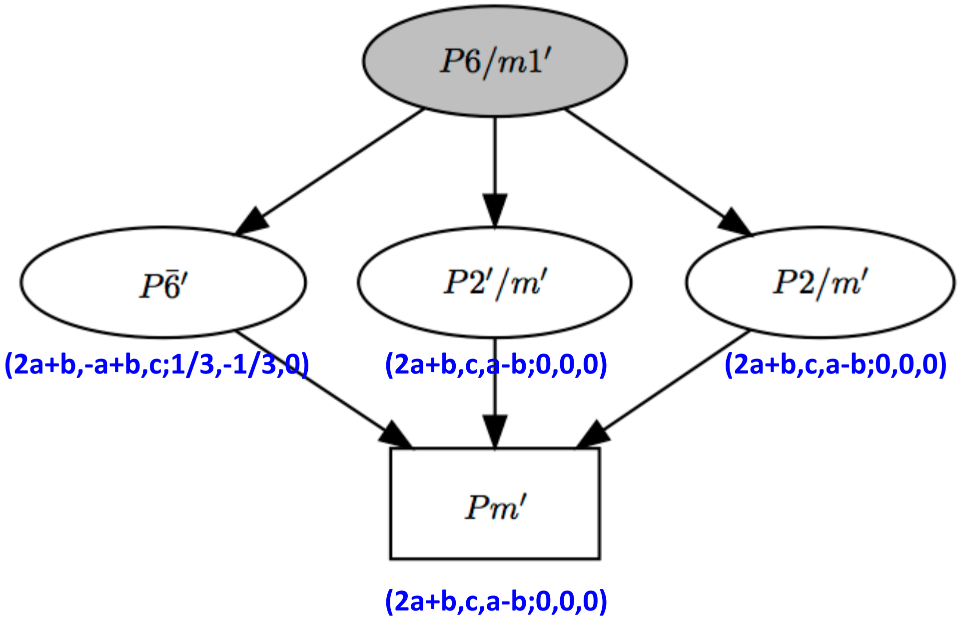

Conclusions

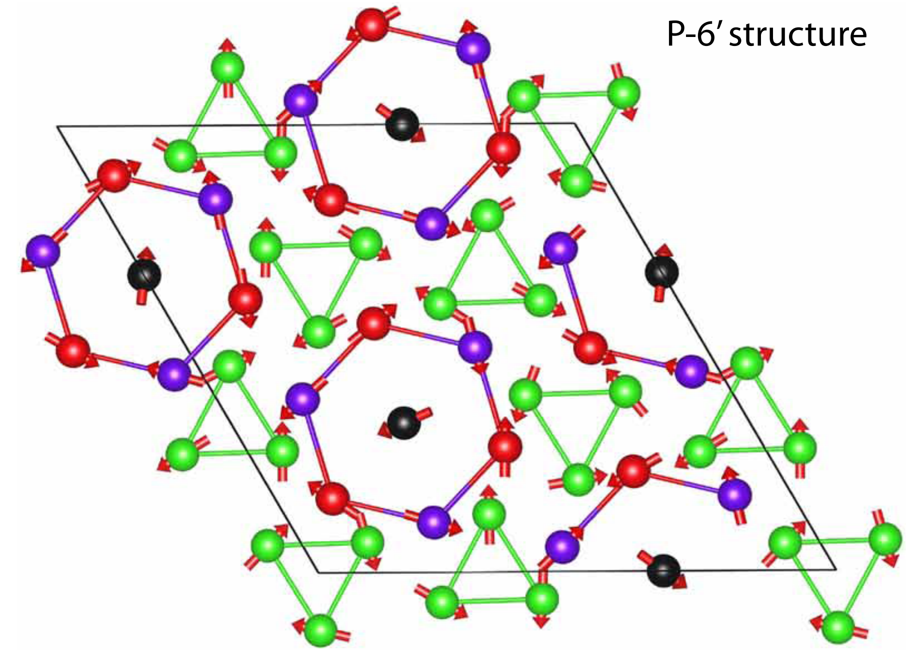

- The antiferromagnetic structure of $Tb_{14}Ag_{51}$ was determined using both magnetic symmetry and irreducible representation arguments.

- The structure given by propagation vector $\mathbf{k}_K$=[1/3,1/3,0] in P6/m is hexagonal magnetic space group (MSG) P-6': maximal possible symmetry for 4D irrep mK4K6.

- P-6' *constrains* the possible mK4K6 ordering that can be present in the structure and implicitly *introduces* third harmonic secondary degrees of freedom associated with propagation vector k = 0 (with weight 34% of k_K) – the modulation is *not sinusoidal*

- 13 independent Tb magnetic moments, all having the same absolute moment value 8.48 (2) μB. 12 Tb – pure cycloid in ab-plane and one with substantial additional helical contribution.

Thank you!

finding unknown complex conjugated (c.c) irrep

c.c is NOT always literal **c.c** of $d(g)$

complex conjugated irrep is

$$d^{c.c}(g) = [d(g_0 g g_0^{-1})]^*$$

where g_0 is element which transforms the arm **k** into the arm −**k**,

irreps of G_k

finding unknown complex conjugated (c.c) irrep

c.c is NOT always literal **c.c** of $d(g)$

complex conjugated irrep is

$$d^{c.c}(g) = [d(g_0 g g_0^{-1})]^*$$

where g_0 is element which transforms the arm **k** into the arm −**k**,

irreps of G_k

P4/nmm (129) **k**1=[0½w]

symop (g)	$W_1(0$★$)$	$W_3(0)$
$1(t_1,t_2,t_3)$	$e^{i\pi(t2+2t3\cdot w)}$	$e^{i\pi(t2+2t3\cdot w)}$
{2_z|½½0}	1	−1
{m_x|½00}	1	1
{m_y|0½0}	1	−1

W3 is **c.c** for W1, η=0, type=3
g_0 is −1

★η=-1,0,1: pseudo-real, complex, real

finding unknown complex conjugated (c.c) irrep

c.c is NOT always literal **c.c** of $d(g)$

complex conjugated irrep is

$$d^{c.c}(g) = [d(g_0 g g_0^{-1})]^*$$

where g_0 is element which transforms the arm **k** into the arm −**k**,

irreps of G_k

P4/nmm (129) **k**1=[0½w]

symop (g)	W1(0★)	W3(0)
1(t1,t2,t3)	$e^{i\pi(t2+2t3\cdot w)}$	$e^{i\pi(t2+2t3\cdot w)}$
{2_z|½½0}	1	−1
{m_x|½00}	1	1
{m_y|0½0}	1	−1

W3 is **c.c** for W1, η=0, type=3
g_0 is −1

P6_5 (170) **k**1=[⅓⅓½]

symop (g)	H1(-1)	H2(0)	H3(0)
1	1	1	
{3+|00⅔}	1	$e^{i2\pi/3}$	$e^{-i2\pi/3}$
{3− |00⅓}	−1	$e^{i\pi/3}$	$e^{-i\pi/3}$

H1 is complex but identical to its c.c.
H2 is **c.c.** for H3
g_0 is 2_{001}

P3c1 (158) **k**1=[⅓⅓½]

symop (g)	H1(-1)	H2(-1)	H3(-1)
1	1	1	1
{3+|000}	1	$e^{i2\pi/3}$	$e^{-i2\pi/3}$
{3− |000}	1	$e^{-i2\pi/3}$	$e^{i2\pi/3}$

All three irreps are complex but identical to themselves η=−1, type=2.
g_0 is m_{110}

★η=-1,0,1: pseudo-real, complex, real

A note: If we use only magnetic symmetry without irreps

too many subgroups to consider and we loose the concept of single irrep active at the transition

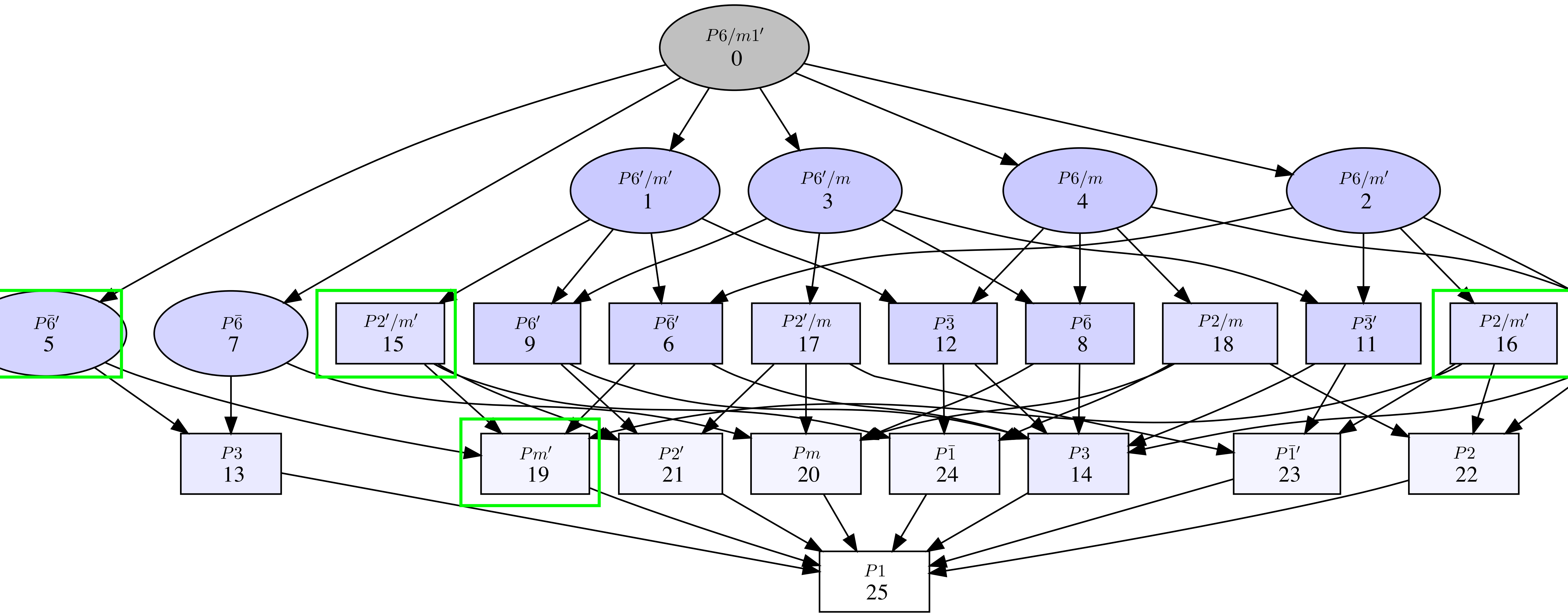

combined fit of both nuclear and magnetic phase

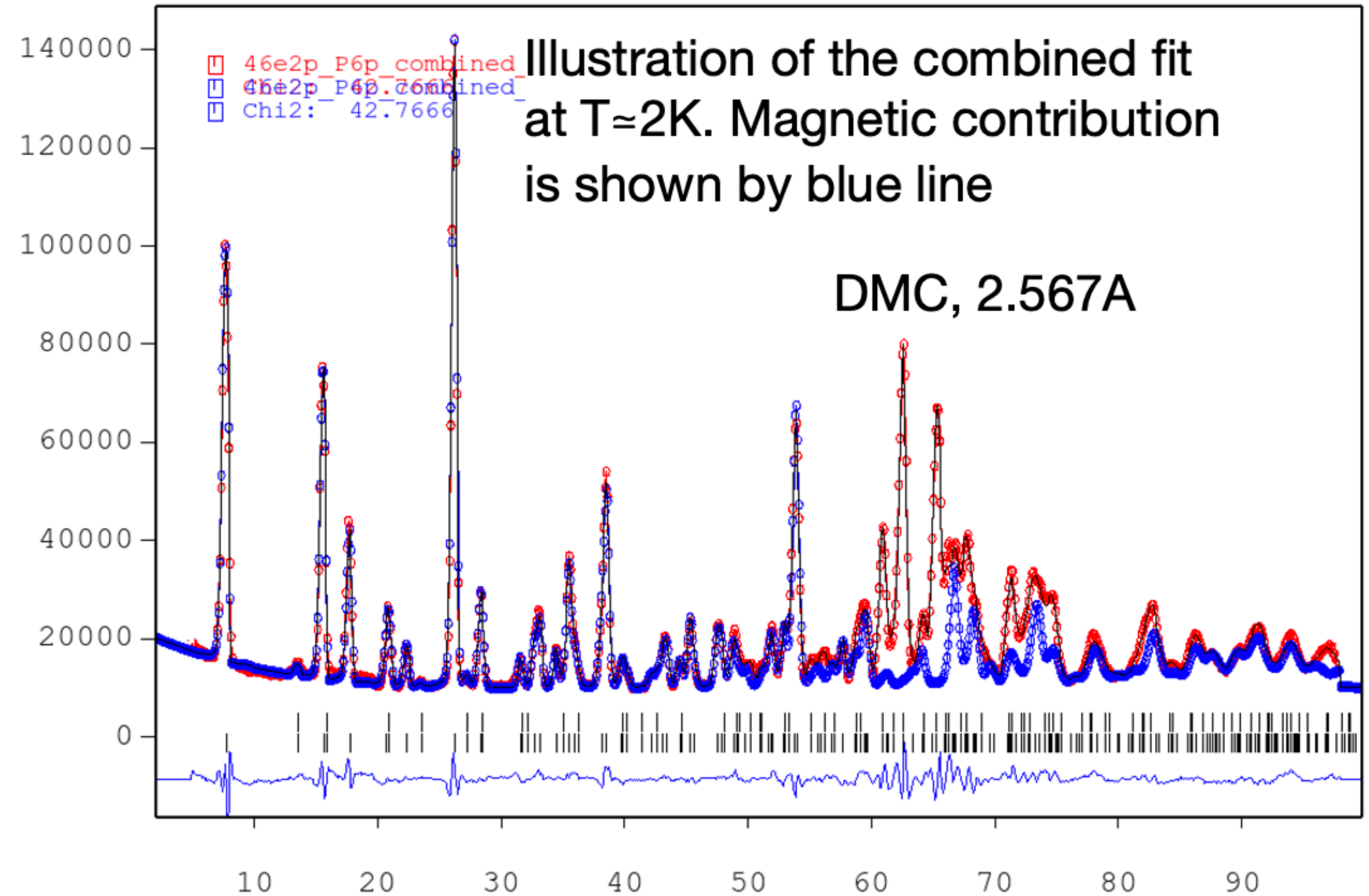

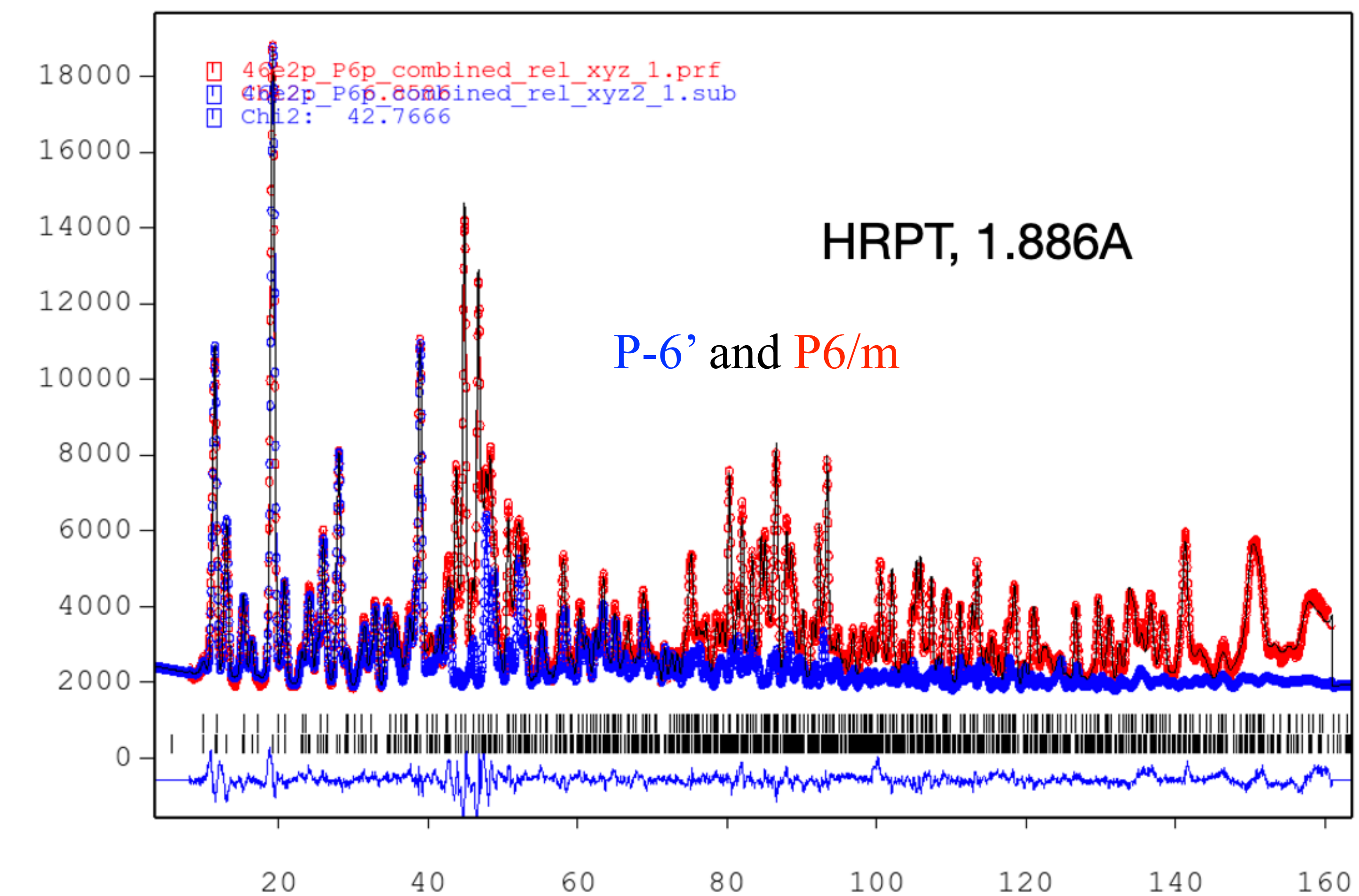

The combined fit with the crystal structure in the space group P6/m converged well, with the atomic positions (19 parameters in total) within less than 1.5 standard deviations from their values in the paramagnetic phase at 30 K for all parameters except four, i.e. 2.3 for x-AG1, 1.9 for y-AG2, 2.0 for y-AG3 and 1.6 for y-AG4. We find these deviations insignificant.

Article | Open Access | Published: 11 September 2020

Visualization of ferroaxial domains in an order-disorder type ferroaxial crystal

T. Hayashida, Y. Uemura, K. Kimura, S. Matsuoka, D. Morikawa, S. Hirose, K. Tsuda, T. Hasegawa & T. Kimura

Nature Communications **11**, Article number: 4582 (2020) | Cite this article

Abstract

Ferroaxial materials that exhibit spontaneous ordering of a rotational structural distortion with an axial vector symmetry have gained growing interest, motivated by recent extensive studies on ferroic materials. As in conventional ferroics (e.g., ferroelectrics and ferromagnetics), domain states will be present in the ferroaxial materials. However, the observation of ferroaxial domains is non-trivial due to the nature of the order parameter, which is invariant under both time-reversal and space-inversion operations. Here we propose that $NiTiO_3$ is an order-disorder type ferroaxial material, and spatially resolve its ferroaxial domains by using linear electrogyration effect: optical rotation in proportion to an applied electric field. To detect small signals of electrogyration (order of 10^{-5} deg V^{-1}), we adopt a recently developed difference image-sensing technique. Furthermore, the ferroaxial domains are confirmed on nano-scale spatial resolution with a combined use of scanning transmission electron microscopy and convergent-beam electron diffraction. Our success of the domain visualization will promote the study of ferroaxial materials as a new ferroic state of matter.

he order parameter characterizing ferroaxial materials is a rotational electric-dipole rrangement[1] and represented by a ferroaxial moment (or ferro-rotation moment) **A** defined s $\mathbf{A} \propto \sum_i \mathbf{r}_i \times \mathbf{p}_i$, where $\mathbf{r}_i$ denotes a position vector of electric dipole $\mathbf{p}_i$ from the ymmetrical center of a structural unit[2,3]. For example, **A** is generated by head-to-tail rrangements of electric dipoles as illustrated in Fig. 1a. The **A** is an axial vector invariant nder both time-reversal and spatial-inversion operations though other symmetries such as a nirror parallel to **A** is broken. The ferroaxial order is closely related to various phenomena ncluding magnetoelectric couplings in multiferroics[4,5,6] and polar vortices in anostructured materials[2,7]. Such an order is sometimes called ferro-rotational order[3,8], and hese terms are often used to describe the existence of rotational distortions inducing finite **A** vith or without a phase transition[4,5,6].

Fig. 1: Ferroaxial order and linear electrogyration induced by ferroaxial order.

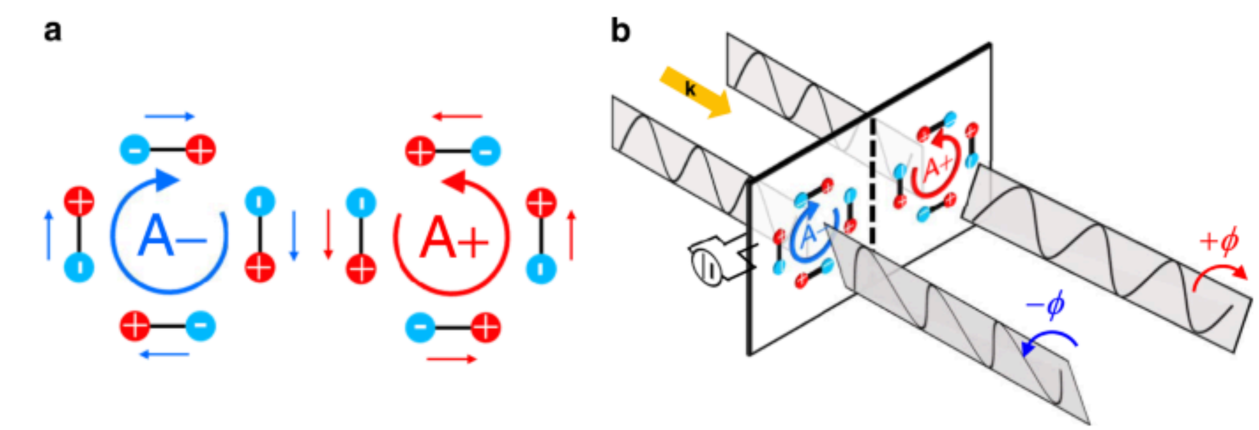

a Ferroaxial moment defined as $\mathbf{A} \propto \sum_i \mathbf{r}_i \times \mathbf{p}_i$, which characterizes ferroaxial materials. Here $\mathbf{r}_i$ denotes a position vector of electric dipole $\mathbf{p}_i$ from the symmetrical center of a structural unit. The

https://en.wikipedia.org/wiki/Electro–optic_effect

https://en.wikipedia.org/wiki/Optical_rotation

https://en.wikipedia.org/wiki/Spin_pumping

https://encyclopedia.pub/entry/36944

https://en.wikipedia.org/wiki/Spintronics

Electric Ferro-Axial Moment as Nanometric Rotator and Source of Longitudinal Spin Current

Satoru Hayami[1], Rikuto Oiwa[2], and Hiroaki Kusunose[2]

[1] *Graduate School of Science, Hokkaido University, Sapporo 060-0810, Japan*
[2] *Department of Physics, Meiji University, Kawasaki 214-8571, Japan*

An electric ferro-axial moment, which is characterized by a nonzero expectation value of a time-reversal-even axial vector, exhibits distinct spatial-inversion and time-reversal properties from conventional ferroelectric, ferromagnetic, and ferro-magnetoelectric orders. Nevertheless, physical properties characteristic of the electric ferro-axial moment have been obscure owing to the absence of its conjugate electromagnetic fields. We theoretically investigate consequences of the presence of the ferro-axial moment on the basis of the symmetry and microscopic model analyses. We show that atomic-scale electric toroidal multipoles are the heart of the ferro-axial moment, which act as a nanometric rotator against external stimuli. Furthermore, we propose an intrinsic generation of a spin current parallel to an applied electric field in both metals and insulators. Our results not only provide a deep microscopic understanding of the role of the ferro-axial moment but also stimulate a new development for functional materials with use of the electric toroidal moment.

Finally, we discuss an intriguing feature of the spin cur- rent under the nonzero ferro-axial moment. Figure 4(a) represents n_e dependence of $\sigma_{xx}^{z(s)}$ at V = 0.7 for θ = π/3

classification of HE

ROY, GUIMARÃES, AND SŁAWIŃSKA PHYSICAL REVIEW MATERIALS **6**, 045004 (2022)

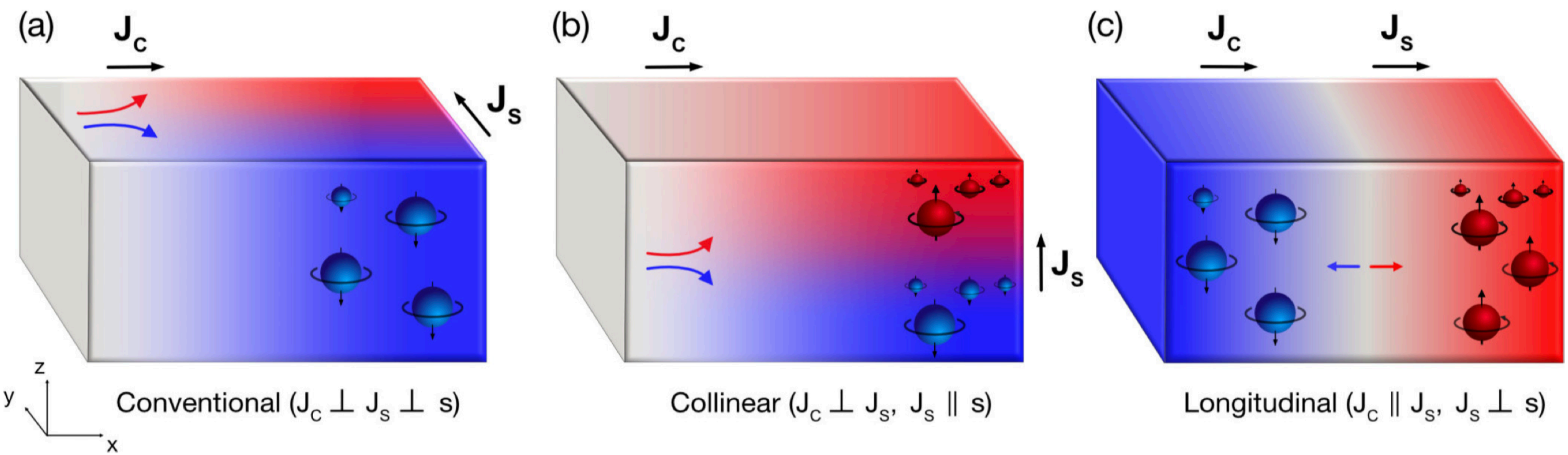

FIG. 1. Classification of the spin Hall effects. We choose the charge current along the x direction and illustrate (a) conventional SHE with spin current along y and spin polarization along z (σ^z_{yx}), (b) collinear SHE with spin current and spin polarization along z (σ^z_{zx}), and (c) a longitudinal spin Hall effect with spin current along x and spin polarization along z (σ^z_{xx}).

[Faraday rotation and electrogyration]

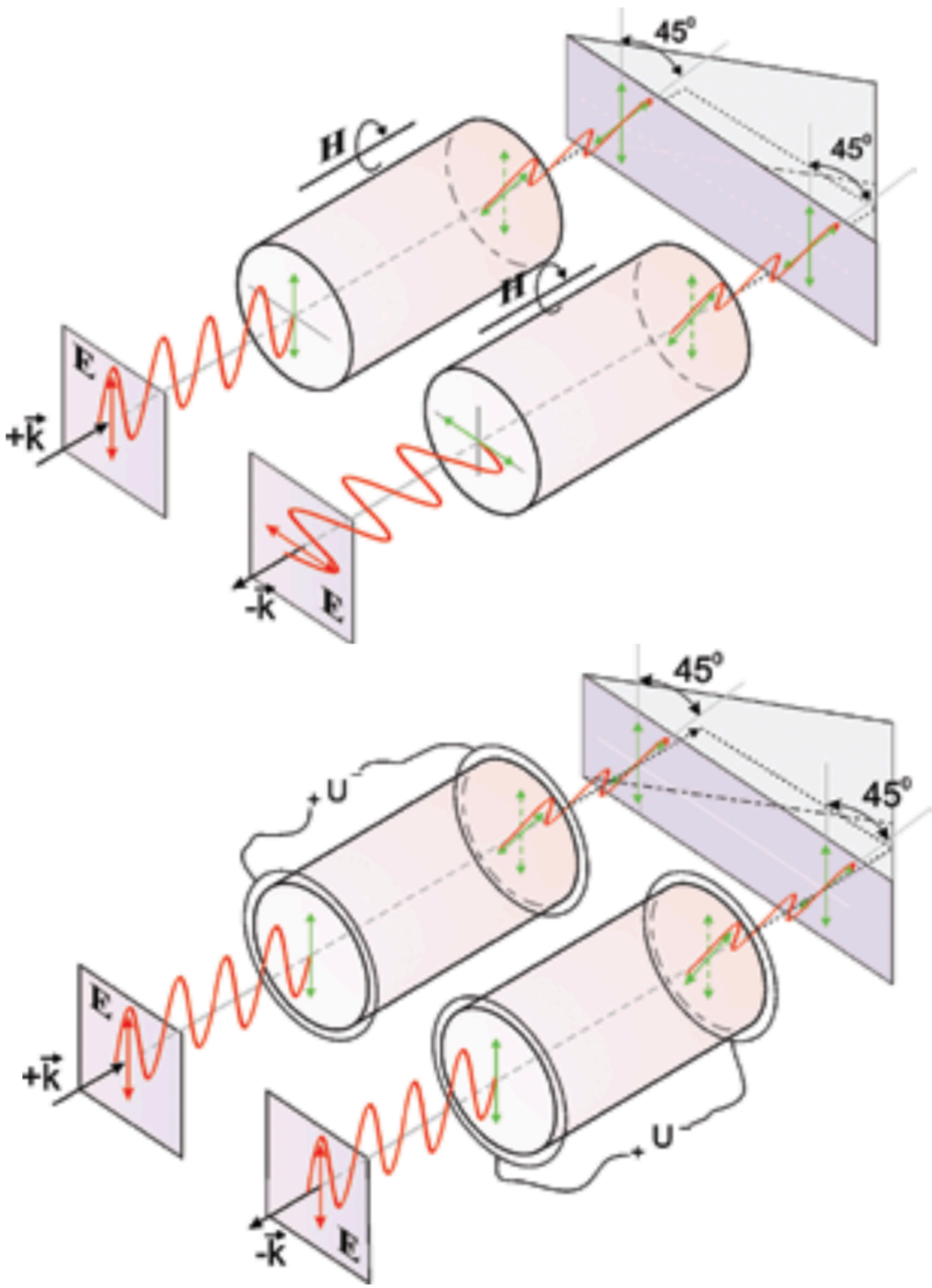

Behaviors of (top) Faraday rotation and (bottom) electrogyration under reversal of the light wave vector.

and the electrogyration rotation is then compensated. This peculiarity also follows from simple mathematical relations: We have $\rho \sim H$ for the Faraday rotation, while the proportion $\rho \sim E \cdot k$ holds true for electrogyration. Thus, the electrogyration

The **Faraday effect** or **Faraday rotation**, sometimes referred to as the **magneto-optic Faraday effect** (**MOFE**),[1] is a physical magneto-optical phenomenon. The Faraday effect causes a polarization rotation which is proportional to the projection of the magnetic field along the direction of the light propagation. Formally, it is a special case of gyroelectromagnetism obtained when the dielectric permittivity tensor is diagonal.[2] This effect occurs in most optically transparent dielectric materials (including liquids) under the influence of magnetic fields.

	Symbol	${}^{*}K_4(0)$
$\begin{pmatrix} 1 & 0 & 0 & t_1 \\ 0 & 1 & 0 & t_2 \\ 0 & 0 & 1 & t_3 \end{pmatrix}$	$\{1\|t_1,t_2,t_3\}$	$\begin{pmatrix} e^{i2\pi(t_1+t_2)/3} & 0 \\ 0 & e^{-i2\pi(t_1+t_2)/3} \end{pmatrix}$
$\begin{pmatrix} 0 & -1 & 0 & 0 \\ 1 & -1 & 0 & 0 \\ 0 & 0 & 1 & 0 \end{pmatrix}$	$\{3^{+}_{001}\|0,0,0\}$	$\begin{pmatrix} e^{i2\pi/3} & 0 \\ 0 & e^{i2\pi/3} \end{pmatrix}$
$\begin{pmatrix} -1 & 1 & 0 & 0 \\ -1 & 0 & 0 & 0 \\ 0 & 0 & 1 & 0 \end{pmatrix}$	$\{3^{-}_{001}\|0,0,0\}$	$\begin{pmatrix} e^{-i2\pi/3} & 0 \\ 0 & e^{-i2\pi/3} \end{pmatrix}$
$\begin{pmatrix} -1 & 0 & 0 & 0 \\ 0 & -1 & 0 & 0 \\ 0 & 0 & 1 & 0 \end{pmatrix}$	$\{2_{001}\|0,0,0\}$	$\begin{pmatrix} 0 & -1 \\ -1 & 0 \end{pmatrix}$
$\begin{pmatrix} 0 & 1 & 0 & 0 \\ -1 & 1 & 0 & 0 \\ 0 & 0 & 1 & 0 \end{pmatrix}$	$\{6^{-}_{001}\|0,0,0\}$	$\begin{pmatrix} 0 & e^{-i\pi/3} \\ e^{-i\pi/3} & 0 \end{pmatrix}$
$\begin{pmatrix} 1 & -1 & 0 & 0 \\ 1 & 0 & 0 & 0 \\ 0 & 0 & 1 & 0 \end{pmatrix}$	$\{6^{+}_{001}\|0,0,0\}$	$\begin{pmatrix} 0 & e^{i\pi/3} \\ e^{i\pi/3} & 0 \end{pmatrix}$
$\begin{pmatrix} -1 & 0 & 0 & 0 \\ 0 & -1 & 0 & 0 \\ 0 & 0 & -1 & 0 \end{pmatrix}$	$\{\bar{1}\|0,0,0\}$	$\begin{pmatrix} 0 & 1 \\ 1 & 0 \end{pmatrix}$
$\begin{pmatrix} 0 & 1 & 0 & 0 \\ -1 & 1 & 0 & 0 \\ 0 & 0 & -1 & 0 \end{pmatrix}$	$\{\bar{3}^{+}_{001}\|0,0,0\}$	$\begin{pmatrix} 0 & e^{i2\pi/3} \\ e^{i2\pi/3} & 0 \end{pmatrix}$
$\begin{pmatrix} 1 & -1 & 0 & 0 \\ 1 & 0 & 0 & 0 \\ 0 & 0 & -1 & 0 \end{pmatrix}$	$\{\bar{3}^{-}_{001}\|0,0,0\}$	$\begin{pmatrix} 0 & e^{-i2\pi/3} \\ e^{-i2\pi/3} & 0 \end{pmatrix}$
$\begin{pmatrix} 1 & 0 & 0 & 0 \\ 0 & 1 & 0 & 0 \\ 0 & 0 & -1 & 0 \end{pmatrix}$	$\{m_{001}\|0,0,0\}$	$\begin{pmatrix} -1 & 0 \\ 0 & -1 \end{pmatrix}$
$\begin{pmatrix} 0 & -1 & 0 & 0 \\ 1 & -1 & 0 & 0 \\ 0 & 0 & -1 & 0 \end{pmatrix}$	$\{\bar{6}^{-}_{001}\|0,0,0\}$	$\begin{pmatrix} e^{-i\pi/3} & 0 \\ 0 & e^{-i\pi/3} \end{pmatrix}$
$\begin{pmatrix} -1 & 1 & 0 & 0 \\ -1 & 0 & 0 & 0 \\ 0 & 0 & -1 & 0 \end{pmatrix}$	$\{\bar{6}^{+}_{001}\|0,0,0\}$	$\begin{pmatrix} e^{i\pi/3} & 0 \\ 0 & e^{i\pi/3} \end{pmatrix}$

G_k #175 $P6/m$ $k = \frac{1}{3}\frac{1}{3}0$

$+2$

$e^{i2\pi/3} = \frac{\sqrt{3}+1)}{2}$

$e^{-i2\pi/3} = \frac{\sqrt{3}-1)}{2}$, $+ = -2$

$\chi(g^2)$

$+2$

$\frac{(i\sqrt{3}-1)^2}{2}$, $\frac{(i\sqrt{3}+1)^2}{2}$, $+ = -2$

$+2$

$\frac{(i\sqrt{3}-1)^2}{2}$, $\frac{(i\sqrt{3}+1)^2}{2}$, $+ = -2$

$\eta = 0$

$h(k) = -k$

-1

$+2$

$e^{-i\pi/3} = \frac{(i\sqrt{3}-1)^2}{2}$

$e^{i\pi/3} = \frac{\sqrt{3}+1)}{2}$, $+ = -2$